

# Glycosylation Analysis of IgLON Family Proteins in Rat Brain by Liquid Chromatography and Multiple-Stage Mass Spectrometry<sup>†</sup>

Satsuki Itoh,<sup>‡</sup> Akiko Hachisuka,<sup>‡</sup> Nana Kawasaki,<sup>\*,‡,§</sup> Noritaka Hashii,<sup>‡</sup> Reiko Teshima,<sup>‡</sup> Takao Hayakawa,<sup>||</sup> Toru Kawanishi,<sup>‡</sup> and Teruhide Yamaguchi<sup>‡</sup>

Division of Biological Chemistry and Biologicals, National Institute of Health Sciences, 1-18-1, Kamiyoga, Setagaya-ku, Tokyo 158-8501, Japan, Core Research for Evolutional Science and Technology of Japan Science and Technology Agency, Kawaguchi Center Building, 4-1-8 Hon-cho, Kawaguchi, Saitama 332-0012, Japan, and Pharmaceutical Research and Technology Institute, Kinki University, 3-4-1 Kowakae, Higashi-Osaka 577-8502, Japan

Received May 23, 2008; Revised Manuscript Received July 17, 2008

**ABSTRACT:** IgLON family proteins, including limbic-associated membrane protein (LAMP), opioid-binding cell adhesion molecule (OBCAM), neurotrimin, and Kilon, are immunoglobulin (Ig) superfamily cell adhesion molecules. These molecules are composed of three Ig domains and a glycosylphosphatidylinositol (GPI) anchor and contain six or seven potential N-glycosylation sites. Although their glycosylations are supposed to be associated with the development of the central nervous system like other Ig superfamily proteins, they are still unknown because of difficulty in isolating individual proteins with a high degree of homology in performing carbohydrate analysis. In this study, we conducted simultaneous site-specific glycosylation analysis of rat brain IgLON proteins by liquid chromatography and multiple-stage mass spectrometry (LC–MS<sup>n</sup>). The rat brain GPI-linked proteins were enriched and separated by sodium dodecyl sulfate–polyacrylamide gel electrophoresis. The four proteins were extracted from the gel, and subjected to LC–MS<sup>n</sup> after proteinase digestions. A set of glycopeptide MS data, including the mass spectrum, the mass spectrum in the selected ion monitoring mode, and the product ion spectra, was selected from all data based on carbohydrate-related ions in the MS/MS spectrum. The peptide portion and the carbohydrate structure were identified on the basis of peptide-related ion and carbohydrate-related ions, and the accurate mass. The site-specific glycosylations of four proteins were elucidated as follows. *N*-Glycans near the N-terminal were disialic acid-conjugated complex- and hybrid-type oligosaccharides. The first Ig domains were occupied by Man-5-9. Diverse oligosaccharides, including Lewis a/x-modified glycans, a brain-specific glycan known as BA-2, and Man-5, were found to be attached to the third Ig domain. Three common structures of glycans were found in the GPI moiety of LAMP, OBCAM, and neurotrimin.

Cell adhesion molecules on cell surfaces are involved in several biological events, such as cell–cell interaction, signaling, and cellular traffic. In the central nervous system, cell adhesion molecules are associated with the differentiation and migration of neurons, and neurite outgrowth. The immunoglobulin (Ig) superfamily, which contains one or more Ig-like domains, is known as one of the cell adhesion molecule families in the central nervous system (1). The Ig superfamily includes various proteins, such as P0, Thy-1, myelin-associated glycoprotein (MAG), neural cell adhesion molecule (NCAM), L1, contactin, and IgLON family proteins. Glycosylation of the Ig superfamily proteins is known

to be involved in cell–cell interactions (2–4). Polysialylated glycans in the fifth domain of NCAM are thought to inhibit the interaction of NCAM with other molecules and to promote neural plasticity through a repulsive interaction (5, 6). The HNK-1 epitope in the third and fifth domains of NCAM is known to mediate molecular recognition in the nervous system (7).

The IgLON superfamily includes the limbic-associated membrane protein (LAMP),<sup>1</sup> the opioid-binding cell adhesion molecule (OBCAM), neurotrimin, and Kilon (8–14), and

<sup>†</sup> This work was supported in part by a Grant-in-Aid from the Ministry of Health and Labor and Welfare, and Core Research for Evolutional Science and Technology Program (CREST) of the Japan Science and Technology Agency (JST).

\* To whom correspondence should be addressed: Division of Biological Chemistry and Biologicals, National Institute of Health Sciences, 1-18-1, Kamiyoga, Setagaya-ku, Tokyo 158-8501, Japan. Telephone: +81-3-3700-9074. Fax: +81-3-3707-6950. E-mail: nana@nihs.go.jp.

<sup>‡</sup> National Institute of Health Sciences.

<sup>§</sup> Core Research for Evolutional Science and Technology of Japan Science and Technology Agency.

<sup>||</sup> Kinki University.

<sup>1</sup> Abbreviations: LC, liquid chromatography; MS, mass spectrometry; MS<sup>n</sup>, multiple-stage mass spectrometry; LAMP, limbic-associated membrane protein; OBCAM, opioid-binding cell adhesion molecule; GlcNAc, *N*-acetylglucosamine; GPI, glycosylphosphatidylinositol; PI-PLC, phosphatidylinositol-specific phospholipase C; PNGase F, peptide *N*-glycosidase F; IT-MS, ion trap mass spectrometer; FT ICR-MS, Fourier transform ion cyclotron resonance mass spectrometer; GCC, graphitized carbon column; TIC, total ion chromatogram; CID, collision-induced dissociation; SIM, selected ion monitoring; dHex, deoxyhexose; Hex, hexose; HexNAc, *N*-acetylhexosamine; Fuc, fucose; Man, mannose; Gal, galactose; GlcNAc, *N*-acetylglucosamine; GlcN, glucosamine; NeuAc, *N*-acetylneuraminic acid; EtNH<sub>2</sub>, ethanolamine; Ino, inositol; BA-2, brain-specific sugar chain, GlcNAcβ1–2Manα1–6(GlcNAcβ1–4)(GlcNAcβ1–2Manα1–3)Manβ1–4GlcNAcβ1–4(Fucα1–6)GlcNAc; SDS–PAGE, sodium dodecyl sulfate–polyacrylamide gel electrophoresis.

LAMP (Q62813)	1:	VRSD---FNR	GT <sup>N12</sup> ITVRQG	DTAILRCVVE	DKNSKVAWL <sup>N38</sup>	RSGIIFAGHD	KWSLDPVEL	EKRHALEYSL	RIQKVDVYDE	GSYTCSVQTQ	HEPKTSQVYL		
OBCAM (P32736)	1:	GVP	VRSGDATFPK	AMD <sup>N17</sup> VTVRQG	ESATLRCTID	DRVTRVAWL <sup>N43</sup>	RSTILYAGND	KWSIDPRVII	LVNTPTQYSI	MIQNVVDVDE	GPYTCSVQTD	NHPKTSRVHL	
neurotrimin (Q62718)	1:		SGDATFPK	AMD <sup>N12</sup> VTVRQG	ESATLRCTID	NRVTRVAWL <sup>N38</sup>	RSTILYAGND	KWCLDPRVVL	LSNTQTQYSI	EIQNVVDVDE	GPYTCSVQTD	NHPKTSRVHL	
Kilon (Q9Z0J8)	1:	VDFP----	WA	AVDN	MLVRKG	DTAVLRCLYE	DGASKGAWL <sup>N26</sup>	RSSIIIFAGGD	KWSVDPRVSI	STLNKRDIYSL	QIQNVVDVDD	GPYTCSVQTQ	HTPRTMQVHL
LAMP	99:	IVQVPPKIS <sup>N108</sup>	ISSDVTNNEG	SN <sup>N120</sup> VTLCMAN	GRPEPVITWR	HLTP-LGREF	EGEEEEYLEIL	GITREQSGKY	ECKAANEVSS	ADVQVK	VTV	NYPPTITESK	
OBCAM	104:	IVQVPPQIM <sup>N113</sup>	ISSDITVNEI	SS	VTLCLAI	GRPEPTVTWR	HLVSKEGGGF	VSEDEYLEIS	DIKRDQSGEY	ECSALNDVAA	PDVRKVK	ITV	NYPPIYSKAK
neurotrimin	99:	IVQVSPKIVE	ISSDISINEG	NN <sup>N120</sup> ISLTLCIAT	GRPEPTVTWR	HISPK-AVG	F	VSEDEYLEIQ	GITREQSGEY	ECSASNDVAA	PVVRV <sup>N184</sup> VTV	NYPPIYSEAK	
Kilon	97:	TVQVPPKIYD	ISNDMTINEG	TN <sup>N118</sup> VTLTCLAT	GKPEPAISWR	HISPS-AKPF	ENGQ-YLDIY	GITRDQAGEY	ECSAENDVSF	PDVKVR	VVV	NFAPTIQEIK	
LAMP	198:	SNEATTGRQA	SLKCEASAVP	APDFEYRDD	TRI-NSANGL	EIKS	TEGQSS	LTVT <sup>N251</sup> VTEEH	YGN <sup>N259</sup> YTCVAAN	KLGV <sup>TN272</sup> ASLV	LFRPGSV-RG	IN <sup>N287</sup>	
OBCAM	204:	NTGVSVGQKG	ILSCEASAVP	MAEFQWFKED	TRLATGLDGV	RIEN	KGRIST	LTFF <sup>N258</sup> VSEKD	YGN <sup>N266</sup> YTCVAATN	KLGN <sup>TN279</sup> ASIT	LYGPGAVIDG	VN <sup>N295</sup>	
neurotrimin	198:	GTGVVPGQKG	TLQCEASAVP	SAEFQWFKDD	KRLVEGKKGV	KVEN	RPFLSR	LTFF <sup>N255</sup> VSEHD	YGN <sup>N260</sup> YTCVASN	KLGH <sup>TN273</sup> ASIM	LFGPGAVSEV	NN <sup>N289</sup>	
Kilon	195:	SGTVTPGRSG	LIRCEGAGVP	PPAFEWYKGE	KRLFNGQQGI	IIQN <sup>N238</sup> FSTRSI	LTVT <sup>N249</sup> VTQEH	FGN <sup>N257</sup> YTCVAAN	KLGT <sup>TN270</sup> ASLP	LNPPSTAQYG	ITG <sup>N287</sup>		

FIGURE 1: Amino acid sequence and potential N-glycosylation sites (in bold) of IgLON family proteins. Their accession numbers in Swiss-prot database are shown in parentheses after their names. The C-terminal amino acids in the proteins are predicted GPI attachment sites.

these proteins are distributed differently in the central nervous system during the development of neurons in a brain (11, 13–18). The IgLON family proteins consist of three Ig domains, the third of which is attached to a glycosylphosphatidylinositol (GPI) anchor. Each of the IgLON family proteins includes six or seven consensus N-glycosylation sites (Figure 1), and the glycosylation is presumed to play essential roles in the neural circuit formation like other Ig superfamily proteins (2–4). However, since the high degree of homology of their amino acid sequences makes it difficult to isolate the individual proteins of this family to perform carbohydrate analysis, their glycosylation features are still unknown with the exception of a linkage of *N*-glycans in OBCAM and Kilon and of high mannose-type and hybrid-type oligosaccharides in LAMP (9, 18, 19).

Recently, liquid chromatography and mass spectrometry (LC–MS) and liquid chromatography and multiple-stage mass spectrometry (LC–MS<sup>n</sup>) have been widely applied to the site-specific glycosylation analysis of a glycoprotein (20–24). Generally, a tryptic digest of an isolated glycoprotein is separated with a reversed-phase or normal-phase column, and the separated glycopeptides are directly subjected to MS and MS<sup>n</sup> (25–27). The site-specific glycosylation is deduced from the mass spectra of the glycopeptides, and the sequences of both the peptide and carbohydrate portions are deduced from the fragment ions in the MS<sup>n</sup> spectra. Using this technique, we previously performed a site-specific glycosylation analysis of rat brain Thy-1, which contains three N-glycosylation sites and a GPI anchor (28). GPI-anchored proteins enriched via phase partitioning with Triton X-114 and PIPLC digestion were separated by SDS–PAGE, and the Thy-1 protein extracted from the gel was digested with trypsin or endoproteinase Asp-N. The Thy-1 glycopeptides were separated and analyzed by using a liquid chromatography and ion trap mass spectrometer (IT-MS) equipped with a C18 column. The peptide portions of glycopeptides were identified on the basis of the *m/z* values of the peptide-related ions and the *b*- and *y*-ions that arose from the peptide backbone. The carbohydrate structures at each glycosylation site and in the GPI moiety were successfully determined from fragment ions in the MS/MS spectra. This result suggests that LC–MS<sup>n</sup> can be effectively utilized for site-specific glycosylation analysis of each glycoprotein in the mixture of several glycoproteins simultaneously.

In this study, we conducted site-specific glycosylation analyses of rat LAMP, OBCAM, neurotrimin, and Kilon using LC–MS<sup>n</sup>. The GPI-linked proteins in the rat brains were separated by SDS–PAGE, and the IgLON family proteins were extracted from a gel band (45–70 kDa). The

mixture of proteins was digested with proteinases, and the site-specific glycosylation analysis of the four proteins was performed by using an ion trap-Fourier transform ion cyclotron resonance mass spectrometer (IT-MS-FT ICR-MS), which is capable of acquiring the accurate mass as well as the MS<sup>n</sup> spectra. We successfully elucidated the site-specific glycosylation and the structure of the GPI moieties of LAMP, OBCAM, neurotrimin, and Kilon. This is the first report of the simultaneous site-specific glycosylation analysis of four similar glycoproteins.

## EXPERIMENTAL PROCEDURES

**Materials.** The rat brains (Wister, male, 3 weeks old) were purchased from Nippon SLC (Hamamatsu, Japan). Phosphatidylinositol-specific phospholipase C (PIPLC) from *Bacillus cereus* was obtained from Molecular Probes (Eugene, OR). Trypsin-Gold was purchased from Promega (Madison, WI). PNGase F and endoproteinase Glu-C were purchased from Roche Diagnostics (Mannheim, Germany). SimplyBlue SafeStain was obtained from Invitrogen (Carlsbad, CA). All other chemicals were of the highest available purity.

**SDS–PAGE of Enriched Lipid-Free GPI-Linked Proteins.** Lipid-free GPI-linked proteins were enriched from rat brain as reported previously (28, 29). Briefly, the homogenate of two rat brains (total wet weight of 1.4 g) was defatted and solubilized with 2% Triton X-114 at 4 °C overnight (29, 30). After centrifugation, the supernatant was subjected to Triton X-114 phase partitioning at 37 °C. Cold acetone was added to the detergent phase containing solubilized membrane proteins, and the resulting precipitate was digested with PIPLC. After the PIPLC digest mixture had been subjected to Triton X-114 phase partitioning, lipid-free GPI-linked proteins in the aqueous phase were precipitated via addition of cold acetone. These proteins were separated by SDS–PAGE (12.5%) (brain wet weight of 50 mg/lane) after carboxamidomethylation (31) and detected after being stained with Coomassie Brilliant Blue G-250 using SimplyBlue SafeStain.

**Protein Identification.** Gel-separated proteins were extracted after in-gel trypsin digestion as previously reported (32) and subjected to LC–MS/MS with a Paradigm MS4 HPLC system (Michrom BioResources, Inc., Auburn, CA) consisting of pump A with 0.1% formic acid and 2% acetonitrile and pump B with 0.1% formic acid and 90% acetonitrile. Peptides were separated with a Magic C18 column (50 mm × 0.2 mm, 3 μm; Michrom BioResources Inc.) with a linear gradient from 5 to 65% of pump B over

20 min at a flow rate of 3  $\mu\text{L}/\text{min}$ . Mass spectra were recorded with a Finnigan LTQ system (Thermo Fisher Scientific, Waltham, MA) using sequential scan events: MS ( $m/z$  450–2000) followed by data-dependent MS/MS on the IT-MS for the most intense ions in positive ion mode. For protein identification, all obtained product ions were subjected to a computer database search analysis with the TurboSEQUEST search engine (Thermo Fisher Scientific) using the Swiss-Prot database and search parameters: a static modification of carboxyamidomethylation (57 Da) at Cys and trypsin for digestion.

**Extraction and Proteinase Digestion of the 45–70 kDa Proteins Separated by SDS–PAGE.** The gel-separated proteins were extracted as previously reported (28). The proteins were extracted with 20 mM Tris-HCl containing 1% SDS by being shaken vigorously overnight after the gel had been broken down into small bits. The extract was filtered with Ultrafree-MC (0.22  $\mu\text{m}$ ; Millipore, Bedford, MA), and the proteins were precipitated via addition of cold acetone. The resulting precipitate was digested with endoproteinase Glu-C (3.75  $\mu\text{g}$ ) in 30  $\mu\text{L}$  of 0.1 M ammonium acetate (pH 8.0) at 37 °C for 4 days, followed by incubation with additional trypsin (1  $\mu\text{g}$ ) at 37 °C overnight.

**LC–MS<sup>n</sup>.** Proteolytic peptides were separated by reversed-phase columns, Magic C30 and C18 (50 mm  $\times$  0.1 mm, 3  $\mu\text{m}$ ; Michrom BioResources), and a graphitized carbon column (GCC), Hypercarb 5  $\mu$  (150 mm  $\times$  0.2 mm; Thermo Fisher Scientific), with a Paradigm MS4 HPLC system consisting of pump A with 0.1% formic acid and 2% acetonitrile and pump B with 0.1% formic acid and 90% acetonitrile. For analysis of glycopeptides, separation was performed with a linear gradient from 5 to 50% pump B over 100 min followed by a 50 to 95% B gradient over 10 min and 95% B over 10 min at a flow rate of 0.5  $\mu\text{L}/\text{min}$ , and mass spectra were recorded with a Finnigan LTQ-FT system (Thermo Fisher Scientific) using sequential scan events: MS ( $m/z$  1000–2000 or 700–2000) with the IT-MS followed by MS with the IT-MS-FT ICR-MS in selected ion monitoring (SIM) mode and data-dependent MS<sup>n</sup> with the IT-MS for the most intense ions. The LC–MS<sup>n</sup> runs were performed with a C30 column and scan range of  $m/z$  1000–2000 (condition A), twice, with a C30 column and scan range of  $m/z$  700–2000 (condition B), once, and with a C18 column and scan range of  $m/z$  1000–2000 (condition C), once. For analysis of GPI-linked peptides, separation was performed with a linear gradient from 5 to 60% pump B over 100 min at a flow rate of 2  $\mu\text{L}/\text{min}$  for a GCC, and mass spectra were recorded with a Finnigan LTQ system using sequential scans: a single mass scan ( $m/z$  700–2000) with the IT-MS followed by data-dependent MS<sup>n</sup> scans with the IT-MS for the most intense ions, twice. LC–MS<sup>n</sup> was performed using a capillary voltage of 1.8 kV and a capillary temperature of 200 °C.

## RESULTS

**Preparation of Lipid-Free IgLON Glycopeptides.** Figure 2 illustrates the experimental procedure for the glycosylation analysis of IgLON family proteins. Lipid-free GPI-linked proteins in a rat brain tissue sample were enriched via phase partitioning with Triton X-114 and PIPLC digestion. The enriched proteins were separated by SDS–PAGE and stained

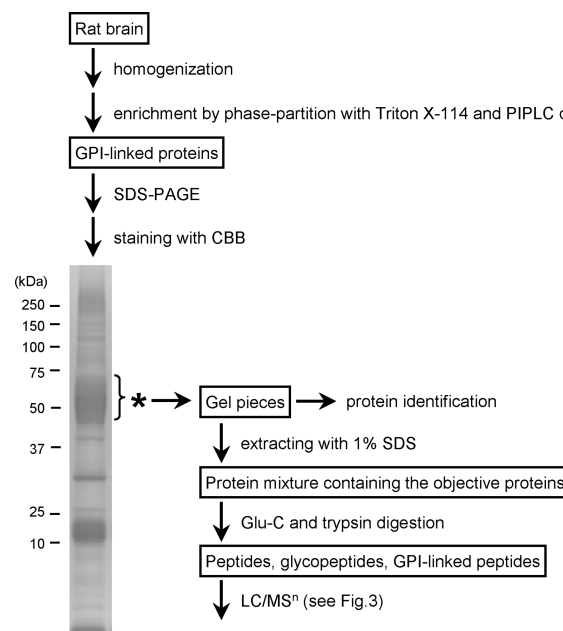


FIGURE 2: Experimental procedure for site-specific glycosylation analysis of IgLON family proteins and SDS–PAGE (12.5%) of lipid-free GPI-linked proteins which were enriched from rat brain. The asterisk indicates the gel band containing IgLON family proteins.

with Coomassie Brilliant Blue. The presence of LAMP, OBCAM, neurotrimin, and Kilon in the gel band at 45–70 kDa was confirmed by in-gel trypsin digestion followed by LC–MS/MS. The IgLON proteins were extracted with other comigrated proteins from 45–70 kDa bands in other lanes by being shaken in 1% SDS. After SDS had been removed, the mixture of proteins was digested with endoproteinase Glu-C and trypsin. Most of the resulting glycopeptides contained only a single N-glycosylation site, with the exception of LGTTN<sup>270</sup>ASLPLNPPSTAQYGITG<sup>287</sup> in Kilon, which included a predicted GPI attachment site at Gly287 in addition to a potential N-glycosylation site at Asn270 (Figure 1). The glycopeptides from IgLON family proteins were separated by using three different columns: a reversed-phase column, a C30 and a C18 column for hydrophobic glycopeptides, and a GCC for hydrophilic glycopeptides, including GPI-linked peptides.

**Glycosylation Analysis of LAMP.** LC–MS analysis was performed via MS on the IT-MS and data-dependent MS in SIM mode on the FT ICR-MS, and data-dependent MS/MS and MS/MS/MS were performed on the IT-MS in the positive ion mode (Figure 3). After MS data acquisition, the MS/MS spectrum (scan  $n$ ) of a glycopeptide was selected manually from all MS data on the basis of the existence of carbohydrate distinctive fragments, such as Hex<sub>1</sub>HexNAc<sub>1</sub><sup>+</sup> ( $m/z$  366) and Hex<sub>1</sub>HexNAc<sub>1</sub>NeuAc<sup>+</sup> ( $m/z$  657). Then a set of the glycopeptide's MS data consisting of the mass spectrum (scan  $n - 2$ ), the mass spectrum in SIM on the FT ICR-MS (scan  $n - 1$ ), the MS/MS spectrum (scan  $n$ ), and the MS/MS/MS spectrum (scan  $n + 1$ ) was selected from all the MS data (step 1). The carbohydrate structure was deduced from the fragment ions appearing in the MS/MS spectrum (scan  $n$ ), and the peptide portion was estimated from the peptide-related ions (step 2). The sequences of some peptides were confirmed by the b- and y-ions that arose from Y<sub>1</sub> ([peptide + HexNAc + H]<sup>+</sup>) in MS/MS/MS (scan  $n +$



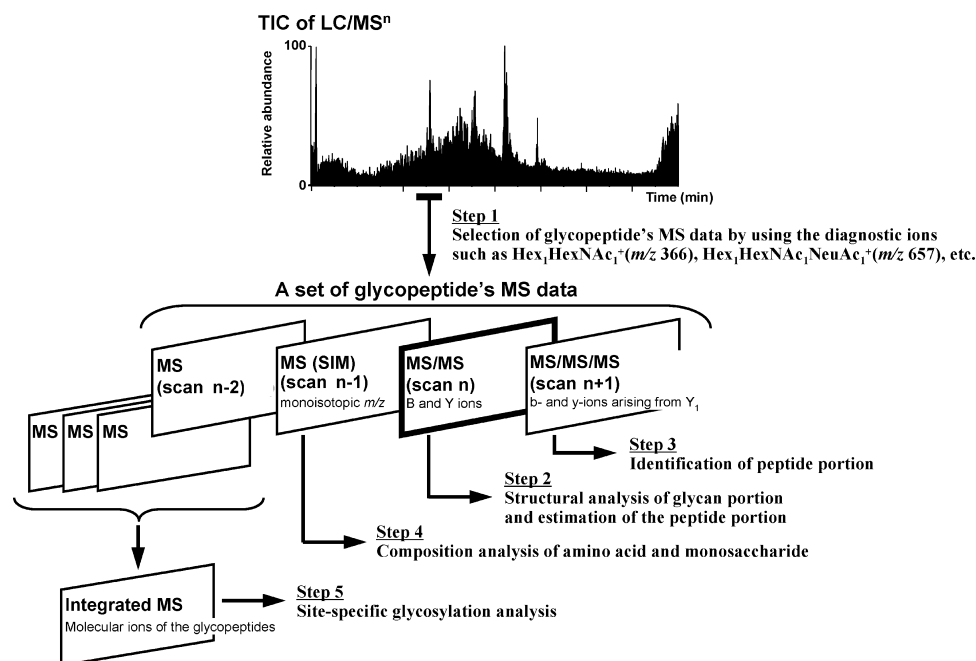


FIGURE 3: Methods used for LC-MS<sup>n</sup> and data analysis.

1) (step 3). The accurate molecular mass that was calculated from the monoisotopic *m/z* value and the charge state acquired by FT ICR-MS in SIM mode (scan *n* - 1) was used to corroborate the assignment of the peptide and glycan moieties (step 4). The mass spectra acquired at the elution position, where the glycopeptides that yielded identical Y<sub>1</sub> ions in the MS/MS and/or MS/MS/MS spectra, were integrated, and the site-specific glycosylation was elucidated on the basis of the distribution of molecular ions in the integrated mass spectra (step 5). As a representative separation pattern, a total ion chromatogram (TIC) obtained by LC-MS<sup>n</sup> with a C30 column (scan range of *m/z* 1000–2000) is shown in Figure 4A. The MS/MS spectra containing the diagnostic ions at *m/z* 366 and 657 were picked out from all the MS data, and the peptides eluted at positions 1–25 were determined to be the glycopeptides on the basis of the carbohydrate-related ions. The 19% of spectra acquired at elution time, including positions 1–25, could be traced back to the glycopeptides of IgLON family proteins.

As for LAMP, it has seven potential N-glycosylation sites at Asn12, -38, -108, -120, -251, -259, and -272, and Asn287 is the predicted site of GPI linkage. On the basis of the presence of the peptide-related ions ([peptide + HexNAc + H]<sup>+</sup>, Y<sub>1</sub> or Y<sub>1α/1β</sub>; or [peptide + dHex-HexNAc + H]<sup>+</sup>, Y<sub>1α</sub>), glycopeptides that were eluted at the positions 1, 11, 14, 12, 4, and 24 were estimated to be the glycopeptides containing Asn12, -38, -108, -251, -259, and -272, respectively. The MS/MS spectra of the glycopeptide containing Asn120 (GSN<sup>120</sup>VTLVCMANGRPE) were not acquired in any of the runs. However, glycosylation at Asn120 was confirmed by the detection of the peptide substituted with Asp (GSD<sup>120</sup>VTLVCMANGRPEPVITWR) after PNGase F digestion (data not shown). Panels A1–F1 of Figure 5 show the representative MS/MS and MS/MS/MS spectra acquired at positions 11, 1, 14, 12, 4, and 24, respectively. The integrated mass spectra of the glycopeptides containing Asn38, -12, -108, -251, -259, and -272 are shown in panels A2–F2 of Figure 5, respectively. The feature of the

glycosylation at each glycosylation site was elucidated on the basis of these MS spectra.

(i) *Asn38* (*Asn43* in *OBCAM* and *Asn38* in *neurotrimin*). Panel A1 of Figure 5 shows one of the MS/MS spectra acquired at position 11. The peptide portion, VAWL(GlcNAc)-N<sup>38</sup>R, was confirmed on the basis of the b- and y-ions that arose from Y<sub>1</sub> (*m/z* 961.5) in the MS/MS/MS spectrum (panel A1'' of Figure 5). A series of doubly charged Y ions with an *m/z* spacing pattern, 81 *m/z* units (Hex), suggests the linkage of Man-7 to this peptide. The attachment of Man-7 to VAWLN<sup>38</sup>R, whose theoretical monoisotopic *m/z* value ([M + 2H]<sup>2+</sup>) is 1149.983, was ascertained by the observed monoisotopic *m/z* value (1149.986) acquired in SIM mode on the FT ICR-MS (panel A1' of Figure 5). Panel A2 of Figure 5 shows the integrated mass spectrum which was obtained from the mass spectra of glycopeptides that yielded Y<sub>1</sub> (*m/z* 961.5) via MS/MS. Four noticeable ion peaks (peaks a-1–a-4) appearing with the differences of 81 *m/z* units are assigned to VAWLN<sup>38</sup>R glycosylated with Man-6-9 (Table 1A). The MS/MS spectra of DKNSKVAWLN<sup>38</sup>R and CVVEDKNSKVAWLN<sup>38</sup>R, which were picked out from positions 9 and 15, also revealed that Man-5, -7, and -8 were attached to Asn38.

(ii) *Asn12*. Panel B1 of Figure 5 shows the representative MS/MS spectrum of glycopeptide, GTDN<sup>12</sup>ITVR, which was selected from position 1. From the Y<sub>1α</sub> ion (*m/z* 1224.5) together with monoisotopic *m/z* value of the molecular ion (*m/z* 1173.132) and a series of doubly charged Y ions with an *m/z* spacing pattern, 146 (NeuAc), 101 (HexNAc), and 81 *m/z* units (Hex), the carbohydrate portion was estimated to be dHex<sub>1</sub>Hex<sub>5</sub>HexNAc<sub>4</sub>NeuAc<sub>4</sub>. Furthermore, a complex-type oligosaccharide, to which one branch of disialic acid was attached, was deduced from the presence of B<sub>4α</sub>/Y<sub>5α'</sub> (*m/z* 495.3), B<sub>2α</sub> (*m/z* 582.7), B<sub>3α</sub> (*m/z* 744.9), B<sub>4α</sub>/Y<sub>5α''</sub> and B<sub>4α</sub>/Y<sub>7α'</sub> (*m/z* 948.2), and B<sub>4α</sub> (*m/z* 1239.5) (inset of panel B1 of Figure 5). The integrated mass spectrum at position 1 suggests that the majority of the glycans at Asn12 are hybrid- and complex-type oligosaccharides containing disialic acids

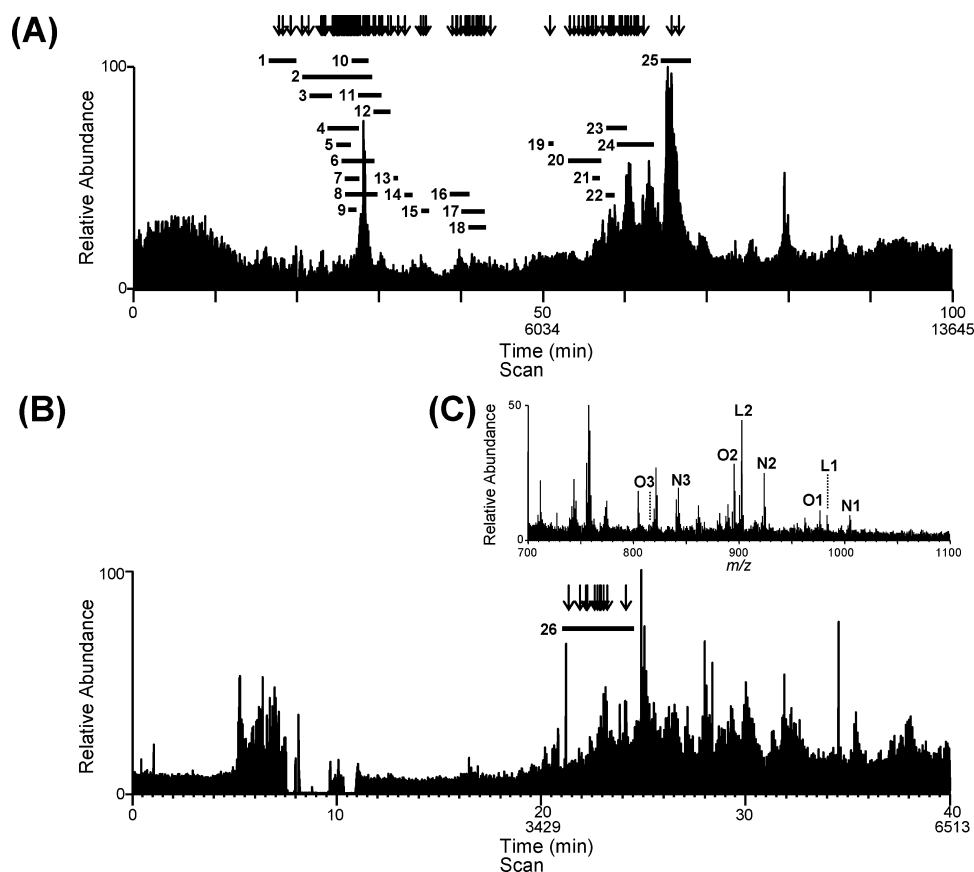


FIGURE 4: Total ion chromatograms obtained by C30-LC-MS<sup>n</sup> (A) and GCC-LC-MS<sup>n</sup> (B). Lines 1–25 and 26 are the elution positions of glycopeptides and GPI-linked peptides, respectively. The down arrow denotes the extracted position of the MS/MS spectra. (C) Integrated mass spectrum obtained from elution position 26. L1 and L2 are molecular ions of GPI-linked peptides from LAMP, N1–N3 those from neurotrimin, and O1–O3 those from OBCAM.

(panel B2 of Figure 5 and Table 1B). In addition, the partial glycosylation at Asn12 was indicated by the detection of nonglycosylated GTDN<sup>12</sup>ITVR.

(iii) *Asn108*. The MS/MS spectrum of glycosylated ISN<sup>108</sup>ISSDVTVNE ( $Y_{1\alpha/1\beta}$ ,  $m/z$  1480.6) acquired at position 14 is shown in panel C1 of Figure 5. The attachment of a Lewis a/x [ $Le^{a/x}$ , Gal-(Fuc)-GlcNAc-] or H antigen (Fuc-Gal-GlcNAc-) motif to the bisected complex-type oligosaccharide was deduced from the monosaccharide composition (dHex<sub>2</sub>Hex<sub>4</sub>HexNAc<sub>5</sub>) and the  $Le^{a/x}$  and H antigen-related ion ( $m/z$  512.1) and  $Y_{1\beta/3\alpha/3\beta}^{2+}$  ( $m/z$  1024.3) (panel C1 of Figure 5, peak c-1 in panel C2 of Figure 5). The alternative LC-MS<sup>n</sup> run with the C30 column (scan range of  $m/z$  1000–2000) suggested that ISN<sup>108</sup>ISSD is also occupied by sialyl  $Le^{a/x}$  (s $Le^{a/x}$ )-modified or core-fucosylated hybrid-type oligosaccharides based on the presence of NeuAc-Hex-(dHex-)HexNAc<sup>+</sup> ( $m/z$  803.1), Hex-(dHex-)HexNAc<sup>+</sup> ( $m/z$  512.3), NeuAc-Hex<sup>+</sup> ( $m/z$  454.2), and [peptide + dHex + HexNAc + H]<sup>+</sup> ( $m/z$  1084.3) (data not shown, Table 1C).

(iv) *Asn251*. The representative MS/MS spectrum of the glycopeptide containing GQSSLTVTN<sup>251</sup>VTE ( $Y_{1\alpha/1\beta}$ ,  $m/z$  1438.6; elution position 12) is shown in panel D1 of Figure 5. From the monoisotopic mass and the  $Le^{a/x}$ -related ions ( $m/z$  350.3 and 512.2), the carbohydrate structure was estimated to be a complex-type oligosaccharide to which the  $Le^{a/x}$  motif was attached (dHex<sub>2</sub>Hex<sub>4</sub>HexNAc<sub>5</sub>; inset of panel D1 of Figure 5). Other glycans at Asn251 were characterized as complex-type oligosaccharides containing s $Le^{a/x}$  or Lewis b/y [ $Le^{b/y}$ , Fuc-Gal-(Fuc)-GlcNAc-] based on the molecular

ions in the integrated mass spectrum (peaks d-1–6 in panel D2 of Figure 5), the s $Le^{a/x}$ -related ions ( $m/z$  803, 657, and 512), and the  $Le^{b/y}$ -related ions ( $m/z$  658.2, 512.1, and 350.2) acquired by the alternative run with the C30 column (scan range of  $m/z$  700–2000) (Table 1D).

(v) *Asn259*. Panel E1 of Figure 5 shows the product ion spectra of HYGN<sup>259</sup>YTCVAANK linked by dHex<sub>1</sub>Hex<sub>3</sub>-HexNAc<sub>5</sub>, which was deduced from the  $Y_{1\alpha/1\beta}$  ion ( $m/z$  1600.6) and the monoisotopic mass acquired at position 4. The BA-2, which is a core-fucosylated and agalactobiantennary oligosaccharide with bisecting GlcNAc, and known as a brain-specific carbohydrate, was suggested by the product ions at  $m/z$  1085.3 (bisecting GlcNAc) and 1746.6 (core-fucosylation) (inset of panel E1 of Figure 5). The majority of other glycans at Asn259 were characterized as  $Le^{a/x}$ -modified complex and hybrid types. Man-5 was suggested to be a minor glycan (panel E2 of Figure 5 and Table 1E).

(vi) *Asn272*. Panel F1 of Figure 5 shows the MS/MS and MS/MS/MS spectra of glycopeptide LGVTN<sup>272</sup>ASLVLFVR ( $Y_{1\alpha/1\beta}$ ,  $m/z$  1492.8), which were acquired at position 24. The monosaccharide composition (dHex<sub>2</sub>Hex<sub>4</sub>HexNAc<sub>5</sub>) and the presence of  $Y_{3\alpha/3\beta}^{2+}$  ( $m/z$  1103.8) and  $Le^{a/x}$ -related ion suggested the attachment of a  $Le^{a/x}$  or H antigen motif to the bisected and core-fucosylated complex-type oligosaccharide (inset of panel F1 of Figure 5). The MS/MS spectra of the LGVTN<sup>272</sup>ASLVLFVRPGSVR glycopeptides ( $Y_{1\alpha/1\beta}^{2+}$ ,  $m/z$  1069) were also picked out at position 24 (data not shown). The  $m/z$  values of molecular ions appearing in the

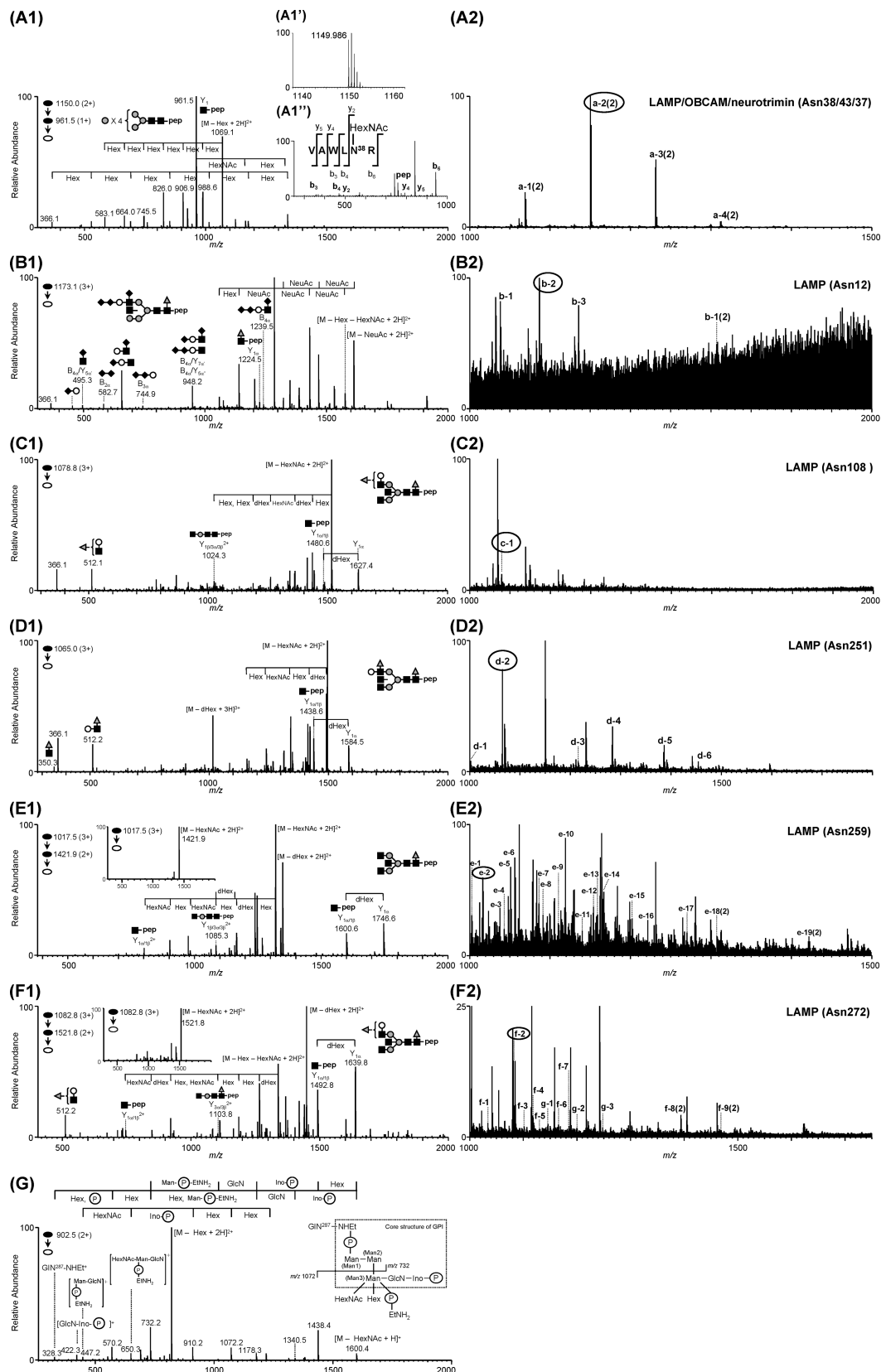


FIGURE 5: MS spectra of LAMP glycopeptides. (A1) MS/MS spectrum of glycopeptide VAWLN<sup>38</sup>R; elution position, 11; precursor ion, [M + 2H]<sup>2+</sup> (*m/z* 1150.0). (A1') Mass spectrum on the FT ICR-MS in SIM mode. (A1'') MS/MS/MS spectrum acquired from Y<sub>1</sub> (*m/z* 961.5). (A2) Integrated mass spectrum obtained from position 11. (B1) MS/MS spectrum of glycopeptide GTDN<sup>12</sup>ITVR; elution position, 1; precursor ion, [M + 3H]<sup>3+</sup> (*m/z* 1173.1). (B2) Integrated mass spectrum at position 1. (C1) MS/MS spectrum of glycopeptide ISN<sup>108</sup>ISSDVTNE; elution position, 14; precursor ion, [M + 3H]<sup>3+</sup> (*m/z* 1078.8). (C2) Integrated mass spectrum at position 14. (D1) MS/MS spectrum of glycopeptide GQSSLTVTN<sup>251</sup>VTE; elution position, 12; precursor ion, [M + 3H]<sup>3+</sup> (*m/z* 1065.0). (D2) Integrated mass spectrum at position 12. (E1) MS/MS and MS/MS/MS spectra of glycopeptide HYGN<sup>259</sup>YTCVAANK; elution position, 4; precursor ion, [M + 3H]<sup>3+</sup> (*m/z* 1017.5). (E2) Integrated mass spectrum at position 4. (F1) MS/MS and MS/MS/MS spectra of glycopeptide LGVTN<sup>272</sup>ASLVLFRR; elution position, 24; precursor ion, [M + 3H]<sup>3+</sup> (*m/z* 1082.8). (F2) Integrated mass spectrum at position 24. (G) MS/MS spectrum of GPI-linked GIN<sup>287</sup>; elution position, 26; precursor ion, [M + 2H]<sup>2+</sup> (*m/z* 902.5). Symbols are as in Figure 9.



Table 1: Continued

peptides		glycopeptides					N-glycan							
protein	sequence <sup>a,b</sup>	elution position	Figure	peak no. <sup>c</sup>	scan in Figure 4A <sup>d</sup>	observed peptide-related ion <sup>e</sup>	observed <i>m/z</i> in SIM mode <sup>b</sup>	theoretical <i>m/z</i> <sup>b</sup>	deduced monosaccharide composition				deduced structure <sup>f</sup> (diagnostic ion)	
									dHex	Hex	HexNAc	NA		
E	HYGN <sup>259</sup> YTCVAANK (1396.619)	4	5, E2	— (B)	801.8(2)	872.021 (3)	872.021 (3)	872.021	0	5	2	0	Man-5	
			e-18 (2)	2884	1600.6	1307.532 (2)	1307.528	1307.528	0	5	2	0	Man-5	
			e-19 (2)	2949 (A)	1601.4	1421.587 (2)	1421.584	1421.584	1	3	4	0	CoreF(1746.7), bisectGN(1085.6)	
			e-1	2891 (A, C)	1600.6	1002.079 (3)	1002.076	1002.076	1	4	4	0	H, CoreF(1746.6), bisectGN(1085.3)	
			e-2	2931 (A, B, C)	1600.6	1015.752 (3)	1015.752 (3)	1015.752	1	3	5	0	C, CoreF(1746.6), bisectGN(1085.3), BA-2 [Figure 5, E1]	
			e-3	2859 (A)	1600.5	1037.089 (3)	1037.086	1037.086	2	5	3	0	H, CoreF(1746.6), 512(512.1)	
			e-4	2840	1600.6	1042.419 (3)	1042.418	1042.418	1	6	3	0	H, 512(512.1)	
			e-5	2878 (A)	1601.6	1050.764 (3)	1050.762	1050.762	2	4	4	0	CoreF(1746.6), L <sup>ax</sup> (350.2, 512.2), bisectGN(1085.5)	
			e-6	2853 (A, B, C)	1600.5	1056.095 (3)	1056.094	1056.094	1	5	4	0	H, CoreF(1747.7), bisectGN(1085.6)	
			e-7	2994	1600.7	1085.433 (3)	1085.432	1085.432	1	5	3	1	H, CoreF(1747.6) or 512(512.2)	
			e-8	2821	1600.5	1091.107 (3)	1091.104	1091.104	2	6	3	0	H, CoreF(1746.6), 512(512.2)	
				— (A, C)	1601.6	1104.779 (3)	1104.780	1104.780	2	5	4	0	H, CoreF(1747.8), bisectGN(1158.7), L <sup>ax</sup> (349.9, 512.3)	
			e-9	2847	1600.6	1110.111 (3)	1110.111	1110.111	1	6	4	0	H, CoreF(1746.6) or L <sup>ax</sup> (350.1, 512.3)	
			e-10	2898 (A, C)	1601.7	1118.457 (3)	1118.455	1118.455	2	4	5	0	C, CoreF(1746.7), bisectGN(1085.7), L <sup>ax</sup> (350.2, 512.1)	
			e-11	2989	1600.7	1139.452 (3)	1139.450	1139.450	1	6	3	1	H, CoreF(1746.7)	
			e-12	2808 (A)	1600.6	1153.467 (3)	1153.466	1153.466	3	5	4	0	C, CoreF(1746.6), L <sup>by</sup> (658.2) or 512/512(512.1/512.3)	
			e-13	2872	1600.4	1158.798 (3)	1158.797	1158.797	2	6	4	0	H, CoreF(1747.7), L <sup>ax</sup> (350.1, 512.1)	
			e-14	3036	1601.7	1166.800 (3)	1166.801	1166.801	1	4	5	1	C, CoreF(1747.4) or 512(512.1), bisectGN(1085.3)	
			e-15	2983	1600.6	1201.813 (3)	1201.811	1201.811	2	5	4	1	C, CoreF(1747.6), sL <sup>ax</sup> (350.1, 512.2, 657.3, 803.2)	
			e-16	2815	1600.6	1221.160 (3)	1221.159	1221.159	3	5	5	0	C, CoreF(1747.6), bisectGN(1085.3), 512(512.2)	
			e-17	3013	1600.7	1269.507 (3)	1269.505	1269.505	2	5	5	1	C, CoreF(1746.7), bisectGN(1085.5), 512(512.1)	



Table 1: Continued

protein	peptides	glycopeptides					N-glycan										
		elution position	Figure	peak no. <sup>c</sup>	scan in Figure 4A <sup>d</sup>	observed peptide-related ion <sup>e</sup>	observed <i>m/z</i> in SIM mode <sup>b</sup>	theoretical <i>m/z</i> <sup>b</sup>	deduced monosaccharide composition								
									dHex	Hex	HexNAc	NA					
F	LGVTN <sup>272</sup> ASLVLF <sup>R</sup> (1288.750)	24	5, F2	— (B)	1492.8	931.109 (3)	1396.160	0	3	5	0	C, bisectGN(1030.9)					
								0	3	5	0	C, bisectGN(1031.0)					
								f-8 (2)	7644 (A, B)	1492.8	1396.161 (2)	1396.160	0	3	5	0	C, bisectGN(1031.0)
													1	3	5	0	C, CoreF(1638.9), bisectGN(1031.2), BA-2
								f-9 (2)	7577 (A, B, C)	1492.7	1469.189 (2)	1469.189	1	3	5	0	C, CoreF(1638.8), bisectGN(1031.2), BA-2
													2	4	4	0	C, CoreF(1640.0), 512(512.3)
								f-1	7558 (A, B, C)	1492.9	1014.806 (3)	1014.806	1	4	5	0	C, bisectGN(1031.1), CoreF(1639.8) or L <sup>ax</sup> (350.2, 512.2)
													1	4	5	0	C, bisectGN(1031.6), CoreF(1640.0) or 512(512.2)
								f-2	7468 (A, B, C)	1492.8	1063.151 (3)	1063.151	1	4	5	0	C, bisectGN(1031.6), CoreF(1638.8), bisectGN(1031.7)
													1	3	6	0	C, CoreF(1638.9)
													0	4	5	1	C, bisectGN(1031.0)
													2	4	5	0	C, CoreF, bisectGN(1103.8) [Figure 5, F1]
													2	4	5	0	C, CoreF(1638.9), bisectGN(1031.0), 512(513.2)
													1	4	6	0	C, bisectGN(1031.2), CoreF(1639.0) or L <sup>ax</sup> (350.3, 512.2)
													1	5	4	1	C, CoreF(1638.8) or sL <sup>ax</sup> (454.2, 512.3, 657.2, 803.1)
													1	5	4	1	H, CoreF(1638.9)
													3	5	4	0	C, CoreF(1639.4), L <sup>by</sup> (512.2, 658.5)
													1	4	5	1	C, CoreF(1638.7), bisectGN(1031.0, 1104.3)
								f-3	7382 (A)	1492.8	1101.510 (3)	1101.506	1	4	6	0	C, CoreF(1639.8), 512(512.2)
													2	4	5	0	C, bisectGN(1031.2), CoreF(1639.0) or L <sup>ax</sup> (350.1, 512.2)
													1	4	6	0	C, bisectGN(1031.2), CoreF(1639.0) or L <sup>ax</sup> (350.3, 512.2)
													1	5	4	1	C, CoreF(1638.8) or sL <sup>ax</sup> (454.2, 512.3, 657.2, 803.1)
1	5	4	1	H, CoreF(1638.9)													
3	5	4	0	C, CoreF(1639.4), L <sup>by</sup> (512.2, 658.5)													
1	4	5	1	C, CoreF(1638.7), bisectGN(1031.0, 1104.3)													
2	5	5	0	C, CoreF(1639.8), 512(512.2)													
2	4	6	0	C, bisectGN(1031.2), CoreF(1639.0) or L <sup>ax</sup> (350.1, 512.2)													
0	5	4	2	C													
f-4	7753 (A, B, C)	1492.7	1117.168 (3)	1117.169	1	5	4	1	C, CoreF(1638.8) or sL <sup>ax</sup> (454.2, 512.3, 657.2, 803.1)								
					1	5	4	1	H, CoreF(1638.9)								
					3	5	4	0	C, CoreF(1639.4), L <sup>by</sup> (512.2, 658.5)								
					1	4	5	1	C, CoreF(1638.7), bisectGN(1031.0, 1104.3)								
					2	5	5	0	C, CoreF(1639.8), 512(512.2)								
					2	4	6	0	C, bisectGN(1031.2), CoreF(1639.0) or L <sup>ax</sup> (350.1, 512.2)								
					0	5	4	2	C								
					2	5	4	1	C, CoreF(1638.7), sL <sup>ax</sup> (453.8, 512.1, 657.1, 803.2)								
					2	5	4	1	C, CoreF(1639.9), 512(512.3)								
					1	5	5	1	C, bisectGN(1032.0), CoreF(1639.3) or 512(512.2)								
f-5	7815 (A, B, C)	1492.6	1165.516 (3)	1165.515	0	5	4	2	C								
					2	5	4	1	C, CoreF(1638.7), sL <sup>ax</sup> (453.8, 512.1, 657.1, 803.2)								
					2	5	4	1	C, CoreF(1639.9), 512(512.3)								
					1	5	5	1	C, bisectGN(1032.0), CoreF(1639.3) or 512(512.2)								
					3	5	5	0	C, CoreF(1639.1), L <sup>by</sup> (512.2, 658.4)								
					2	5	6	0	C, CoreF(1638.9), L <sup>ax</sup> (350.2, 512.2)								
					1	5	4	2	C, CoreF(1639.8)								
					1	5	5	1	C, bisectGN(1032.0), CoreF(1639.3) or 512(512.2)								
					3	5	5	0	C, CoreF(1639.1), L <sup>by</sup> (512.2, 658.4)								
					2	5	6	0	C, CoreF(1638.9), L <sup>ax</sup> (350.2, 512.2)								
f-6	7889 (A, C)	1492.8	1130.846 (3)	1130.845	1	4	5	1	C, CoreF(1638.7), bisectGN(1031.0, 1104.3)								
					2	5	5	0	C, CoreF(1639.8), 512(512.2)								
					2	4	6	0	C, bisectGN(1031.2), CoreF(1639.0) or L <sup>ax</sup> (350.1, 512.2)								
					0	5	4	2	C								
					2	5	4	1	C, CoreF(1638.7), sL <sup>ax</sup> (453.8, 512.1, 657.1, 803.2)								
					2	5	4	1	C, CoreF(1639.9), 512(512.3)								
					1	5	5	1	C, bisectGN(1032.0), CoreF(1639.3) or 512(512.2)								
					3	5	5	0	C, CoreF(1639.1), L <sup>by</sup> (512.2, 658.4)								
					2	5	6	0	C, CoreF(1638.9), L <sup>ax</sup> (350.2, 512.2)								
					1	5	4	2	C, CoreF(1639.8)								
f-7	7765	1493.9	1184.864 (3)	1184.862	1	5	5	1	C, bisectGN(1032.0), CoreF(1639.3) or 512(512.2)								
					3	5	5	0	C, CoreF(1639.1), L <sup>by</sup> (512.2, 658.4)								
					2	5	6	0	C, CoreF(1638.9), L <sup>ax</sup> (350.2, 512.2)								
					1	5	4	2	C, CoreF(1639.8)								
					1	5	5	1	C, bisectGN(1032.0), CoreF(1639.3) or 512(512.2)								
					3	5	5	0	C, CoreF(1639.1), L <sup>by</sup> (512.2, 658.4)								
					2	5	6	0	C, CoreF(1638.9), L <sup>ax</sup> (350.2, 512.2)								
					1	5	4	2	C, CoreF(1639.8)								
					1	5	5	1	C, bisectGN(1032.0), CoreF(1639.3) or 512(512.2)								
					3	5	5	0	C, CoreF(1639.1), L <sup>by</sup> (512.2, 658.4)								
2	5	6	0	C, CoreF(1638.9), L <sup>ax</sup> (350.2, 512.2)													
f-8	7765	1493.2	1214.201 (3)	1214.201	1	5	4	2	C, CoreF(1639.8)								
					1	5	4	2	C, CoreF(1639.8)								
					1	5	4	2	C, CoreF(1639.8)								
					1	5	4	2	C, CoreF(1639.8)								
					1	5	4	2	C, CoreF(1639.8)								
					1	5	4	2	C, CoreF(1639.8)								
					1	5	4	2	C, CoreF(1639.8)								
					1	5	4	2	C, CoreF(1639.8)								
					1	5	4	2	C, CoreF(1639.8)								
					1	5	4	2	C, CoreF(1639.8)								

Table 1: Continued

peptides		glycopeptides					N-glycan						
protein	sequence <sup>a,b</sup>	elution position	Figure	peak no. <sup>c</sup>	scan in Figure 4A <sup>d</sup>	observed peptide-related ion <sup>e</sup>	observed <i>m/z</i> in SIM mode <sup>b</sup>	theoretical <i>m/z</i> <sup>b</sup>	deduced monosaccharide composition				deduced structure <sup>f</sup> (diagnostic ion)
									dHex	Hex	HexNAc	NA	
OBCAM	AMDN <sup>17</sup> VTVR (904.444)	2	6, A2	h-1	2408 (A)	1254.5	1018.407 (3)	1018.405	1	5	3	2	H, CoreF(1254.5), diSia(583.0)
						1254.7	1086.098 (3)	1086.099	1	5	4	2	CoreF(1254.7)
						1254.5	1628.644 (2)	1628.644	1	5	4	2	C, CoreF(1254.5)
						1254.7	1115.437 (3)	1115.437	1	5	3	3	H, CoreF(1254.7), diSia(583.0)
						1254.5	1672.651 (2)	1672.652	1	5	3	3	H, CoreF(1254.5), diSia(583.3)
						1254.6	1169.454 (3)	1169.455	1	6	3	3	H, CoreF(1254.6), diSia(583.0)
						1254.5	1183.131 (3)	1183.130	1	5	4	3	H, CoreF(1254.5) or 512(512.2), diSia(582.6)
						<b>1254.5</b>	<b>1280.163 (3)</b>	<b>1280.162</b>	<b>1</b>	<b>5</b>	<b>4</b>	<b>4</b>	<b>C, CoreF(1254.5), diSia(582.9) [Figure 6, A1]</b>
						1108.6	1377.198 (3)	1377.194	1	5	4	5	Man-5
						961.5	987.930 (2)	987.930	0	5	2	0	Man-6
						961.5	1068.956 (2)	1068.957	0	6	2	0	Man-6
						<b>961.5</b>	<b>1149.986(2)</b>	<b>1149.983</b>	<b>0</b>	<b>7</b>	<b>2</b>	<b>0</b>	<b>Man-7 [Figure 5, A1]</b>
961.5	1231.010 (2)	1231.010	0	8	2	0	Man-8						
961.5	1312.039 (2)	1312.036	0	9	2	0	Man-9						
		—	—	—	—	—	—	glycosylated <sup>g</sup>					
		—	—	—	—	—	—	glycosylated <sup>g</sup>					
H	VHLIVQVPPQIMN <sup>11</sup> 3ISSD (1889.008)	—	—	—	—	—	—	—	—	—	—	—	CoreF(1606.3), bisectGN(1087.8)
	VHLIVQVPPQIMN <sup>11</sup> 3ISSDITVNE (2445.294)	—	—	—	—	—	—	—	—	—	—	—	C, CoreF(1606.5), bisectGN(1088.6), BA-2
	ISTLTFFN <sup>28</sup> VSE (1256.629)	25	6, B2	—	(B)	1460.5	969.088 (3)	969.088	1	3	5	0	C, CoreF(1606.5), bisectGN(1088.6), BA-2
			—	(A, C)	1461.5	1453.128 (2)	1453.128	1	3	5	0	0	C, CoreF(1606.5), bisectGN(1088.4), BA-2

Table 1: Continued

protein	peptides	glycopeptides					N-glycan							
		sequence <sup>a,b</sup>	elution position	Figure	peak no. <sup>c</sup>	scan in Figure 4A <sup>d</sup>	observed peptide-related ion <sup>e</sup>	observed <i>m/z</i> in SIM mode <sup>b</sup>	theoretical <i>m/z</i> <sup>b</sup>	deduced monosaccharide composition				
										dHex	Hex	HexNAc	NA	deduced structure <sup>f</sup> (diagnostic ion)
I	YGN <sup>266</sup> YTCVATNK (1289.571)	7	6, C2							2	4	5	0	C, CoreF(1606.5), L <sup>ax</sup> (350.1, 512.2) or (L <sup>by</sup> 658.4)
										2	4	5	0	C, 512(512.3)
										1	4	5	1	C, CoreF(1606.5)
										2	5	4	1	C, CoreF(1606.6) (sL <sup>ax</sup> 349.2, 512.2, 804.1)
										3	5	5	0	C, CoreF(1606.5), L <sup>by</sup> (350.7, 512.3, 658.2)
										1	4	6	1	C, CoreF(1606.6) or sL <sup>ax</sup> (350.1, 512.5, 657.1, 803.1)
										2	5	5	1	C, CoreF(1606.5), sL <sup>ax</sup> (454.0, 512.2, 803.2)
										2	5	6	1	C, CoreF(1606.6) (sL <sup>ax</sup> 454.2, 512.2, 657.1, 803.3) [Figure 6, B1]
										3	6	6	1	C, CoreF(1606.5), 512(512.2)
										0	5	2	0	Man-5
										1	3	4	0	CoreF(1639.6), bisectGN(1031.5)
										1	3	5	0	C, CoreF(1639.6), bisectGN(1032.2), BA-2
										1	3	5	0	C, CoreF(1639.6), bisectGN(1105.0), BA-2
										2	4	4	0	CoreF(1639.5), L <sup>ax</sup> (350.2, 512.1), bisectGN(1105.1)
										2	4	5	0	C, CoreF(1640.5), L <sup>ax</sup> (350.4, 512.2), bisectGN(1105.9) [Figure 6, C1]
										3	5	4	0	H, CoreF(1639.5), L <sup>by</sup> (350.3, 512.1, 658.1)
										3	5	5	0	C, CoreF(1639.6), L <sup>ax</sup> (349.0, 512.1), bisectGN(1032.7)
										0	5	2	0	Man-5
										1	3	5	0	C, CoreF(1754.5), bisectGN(1089.6), BA-2
										1	3	5	0	C, CoreF(1754.6), bisectGN(1089.1), BA-2
	DYGN <sup>266</sup> YTCVATNK (1404.598)	13	—							2	4	5	0	C, CoreF(1754.7), L <sup>ax</sup> (350.3, 512.3)
										3	5	4	0	H, CoreF(1754.8), 512(512.2)
										1	3	4	0	CoreF(1882.8), bisectGN(1225.1)
										1	3	5	0	C, CoreF(1884.9), bisectGN(1226.7), BA-2
										2	5	4	0	H, CoreF(1883.8), L <sup>ax</sup> (350.4, 512.2)
										0	5	2	0	Man-5
										3	5	4	0	H, CoreF(1639.5), L <sup>by</sup> (350.3, 512.1, 658.1)
										3	5	5	0	C, CoreF(1639.6), L <sup>ax</sup> (349.0, 512.1), bisectGN(1032.7)
										0	5	2	0	Man-5
										1	3	5	0	C, CoreF(1754.5), bisectGN(1089.6), BA-2
	KDYGN <sup>266</sup> YTCVATNK (1532.693)	6	—							1	3	4	0	CoreF(1882.8), bisectGN(1225.1)
										1	3	5	0	C, CoreF(1884.9), bisectGN(1226.7), BA-2
										1	3	5	0	H, CoreF(1883.8), L <sup>ax</sup> (350.4, 512.2)
										2	5	4	0	H, CoreF(1883.8), L <sup>ax</sup> (350.4, 512.2)
										2	5	4	0	H, CoreF(1883.8), L <sup>ax</sup> (350.4, 512.2)

Table 1: Continued

peptides			glycopeptides					N-glycan						
protein	sequence <sup>a,b</sup>	elution position	Figure	peak no. <sup>c</sup>	scan in Figure 4A <sup>d</sup>	observed peptide-related ion <sup>e</sup>	observed <i>m/z</i> in SIM mode <sup>b</sup>	theoretical <i>m/z</i> <sup>b</sup>	deduced monosaccharide composition				deduced structure <sup>f</sup> (diagnostic ion)	
									dHex	Hex	HexNAc	NA		
J	LGNTN <sup>279</sup> ASITLYGPGAVID (1774.910)	—	—	—	— (C)	1736.5	1163.814 (3)	1163.813	2	4	5	0	C, CoreF(1882.7), bisectGN(1153.7), L <sup>NA</sup> s (350.3, 512.2)	
						1737.6	1198.826 (3)	1198.823	3	5	4	0	C, CoreF(1884.7), L <sup>NA</sup> s (350.1, 512.2)	
						1737.1	1212.160 (3)	1212.159	1	4	5	1	C, CoreF(1883.9), bisectGN(1226.3)	
						1737.0	1247.170 (3)	1247.169	2	5	4	1	CoreF(1882.8), sL <sup>NA</sup> s (453.8, 512.2, 657.2, 803.2)	
						1978.7	1093.161 (3)	1093.162	0	3	5	0	C	
						1979.8	1141.848 (3)	1141.848	1	3	5	0	C, CoreF(1062.9), bisectGN(1273.8), BA-2	
						1254.5	1018.407 (3)	1018.405	1	5	3	2	H, CoreF(1254.5), diSia(583.0)	
						1254.7	1086.098 (3)	1086.099	1	5	4	2	CoreF(1254.7)	
						1254.5	1628.644 (2)	1628.644	1	5	4	2	C, CoreF(1254.5)	
						1254.7	1115.437 (3)	1115.437	1	5	3	3	H, CoreF(1254.7), diSia(583.0)	
neurotrimin	G AMDN <sup>12</sup> VTVR (904.444)	2	6, A2	h-1	2408 (A)	1979.8	1141.848 (3)	1141.848	1	3	5	0	C, CoreF(1062.9), bisectGN(1273.8), BA-2	
						1254.5	1018.407 (3)	1018.405	1	5	3	2	H, CoreF(1254.5), diSia(583.0)	
						1254.7	1086.098 (3)	1086.099	1	5	4	2	CoreF(1254.7)	
						1254.5	1628.644 (2)	1628.644	1	5	4	2	C, CoreF(1254.5)	
						1254.7	1115.437 (3)	1115.437	1	5	3	3	H, CoreF(1254.7), diSia(583.0)	
						1254.5	1672.651 (2)	1672.652	1	5	3	3	H, CoreF(1254.5), diSia(583.3)	
						1254.6	1169.454 (3)	1169.455	1	6	3	3	H, CoreF(1254.6), diSia(583.0)	
						1254.5	1183.131 (3)	1183.130	1	5	4	3	H, CoreF(1254.5) or 512(512.2), diSia(582.6)	
						1254.5	1280.163 (3)	1280.162	1	5	4	4	C, CoreF(1254.5), diSia(582.9) [Figure 6, A1]	
						1108.6	1377.198 (3)	1377.194	1	5	4	5	Man-5	
A	VAWLN <sup>38</sup> R (757.424)	11	5, A2	*	— (C)	961.5	987.930 (2)	987.930	0	5	2	0	Man-5	
						961.5	1068.956 (2)	1068.957	0	6	2	0	Man-6	
						3523 (A, B, C)	1149.986(2)	1149.983	0	7	2	0	Man-7 [Figure 5, A1]	
						3364 (A, B, C)	1231.010 (2)	1231.010	0	8	2	0	Man-8	
						3221 (A, B, C)	961.5	1231.010 (2)	1231.010	0	8	2	0	Man-9
						3413 (A, B, C)	961.5	1312.039 (2)	1312.036	0	9	2	0	glycosylated <sup>g</sup>
						—	—	—	—	—	—	—	glycosylated <sup>g</sup>	
						—	—	—	—	—	—	—	glycosylated <sup>g</sup>	
						—	—	—	—	—	—	—	glycosylated <sup>g</sup>	
						K	LTFFN <sup>252</sup> VSE (955.465)	20	7, A2	k-4 (2)	6885 (A)	1159.4	1086.954 (2)	1086.951
1159.4	1180.493 (2)	1180.494	1	4	3							0	CoreF(1305.5)	
1159.4	1201.011 (2)	1201.007	1	3	4							0	CoreF(1305.4)	
1159.5	1261.520 (2)	1261.520	1	5	3							0	H, CoreF(1305.3)	
1159.4	1302.551 (2)	1302.546	1	3	5							0	C, CoreF(1305.3), bisectGN(864.6), BA-2	
1159.5	1334.551 (2)	1334.549	2	5	3							0	H, CoreF(1305.3), 512(512.3)	
1159.4	1355.062 (2)	1355.062	2	4	4							0	CoreF(1305.2), 512(512.4)	
1159.5	1363.059 (2)	1363.060	1	5	4							0	H, bisectGN(864.4), CoreF(1305.4) or 512(511.9)	
1160.4	1407.068 (2)	1407.068	1	5	3							1	H, CoreF(1306.4)	
1159.8	1415.576 (2)	1415.575	2	6	3							0	H, CoreF(1305.3)	





Table 1: Continued																	
protein	peptides		glycopeptides					N-glycan									
	sequence <sup>a,b</sup>	elution position	Figure	peak no. <sup>c</sup>	scan in Figure 4A <sup>d</sup>	observed peptide-related ion <sup>e</sup>	observed m/z in SIM mode <sup>b</sup>	theoretical m/z <sup>b</sup>	deduced monosaccharide composition								
									dHex	Hex	HexNAc	NA	deduced structure/ (diagnostic ion)				
M	LGHTN <sup>273</sup> ASIMLEFGPGAVSE (1799.888)	23	7, C2	m-1	— (C)	1732.7	1197.144 (3)	1197.139	3	5	4	0	H, CoreF(1877.7), L <sup>by</sup> (512.2, 658.2), bisectGN(1149.1)				
						1731.7	1210.475 (3)	1210.475	1	4	5	1	C, CoreF(1877.8), bisectGN(1222.6)				
						1732.8	1245.488 (3)	1245.485	2	5	4	1	H, CoreF(1879.7), sL <sup>ax</sup> (453.9, 512.2, 657.2, 803.3)				
						1732.7	1264.834 (3)	1264.833	3	5	5	0	C, CoreF(1878.7), bisectGN(1223.4), 512(512.1)				
						1731.9	1293.835 (3)	1293.831	1	5	4	2	H, CoreF(1877.6), bisectGN(1150.5)				
						1731.9	1294.175 (3)	1294.171	3	5	4	1	C, CoreF(1877.7)				
						1002.6(2)	1101.491 (3)	1101.488	0	3	5	0	C, bisectGN(1286.7) [Figure 7, C1]				
						1003.1(2)	1141.835 (3)	1141.830	0	5	4	0	H, bisectGN(1286.5)				
						1002.6(2)	1150.176 (3)	1150.174	1	3	5	0	C, CoreF(1075.6), bisectGN(1357.6), BA-2				
						1002.7(2)	1190.520 (3)	1190.516	1	5	4	0	H, CoreF(1075.4) or 512(512.0), bisectGN(1359.1)				
Kilon	N	GAWLN <sup>36</sup> R (715.377)	8, A2	m-4	7186	1002.8(2)	1244.537 (3)	1244.534	1	6	4	0	H, 512(512.2)				
					— (B)	919.5	966.907 (2)	966.907	0	5	2	0	Man-5				
					n-1 (2)	2664 (A, B, C)	919.5	1047.934 (2)	1047.933	0	6	2	0	Man-6 [Figure 8, A1]			
					n-2 (2)	2706 (A, B, C)	919.5	1128.960 (2)	1128.960	0	7	2	0	Man-7			
					n-3 (2)	2679 (A, B, C)	919.4	1209.988 (2)	1209.986	0	8	2	0	Man-8			
					—	5234	972.3	1040.101 (3)	1040.102	0	6	2	0	Man-6			
					8, B2	o-1	4760	1765.8	1070.475 (3)	1070.472	1	3	5	0	C, CoreF(1910.8), bisectGN(1167.3), BA-2 [Figure 8, B1]		
					o-2	4683	1764.7	1105.485 (3)	1105.483	2	4	4	0	CoreF(1910.9), bisectGN(1167.8), 512(512.2)			
					o-3	4710 (C)	1765.7	1173.176 (3)	1173.176	2	4	5	0	C, CoreF(1911.9), bisectGN(1167.3), 512(512.1)			
					o-4	4638	1765.8	1275.880 (3)	1275.879	3	5	5	0	C, CoreF(1910.9), 512(512.1)			
P	LFNGQQGHIIQN <sup>238</sup> FSTR (1834.969) RLFNQQQGHIIQN <sup>238</sup> FSTR (1991.070) KRLFNQQQGHIIQN <sup>238</sup> FSTR (2119.165)	22	8, C2	p-1	— (C)	1764.9	1401.911 (3)	1401.910	1	5	4	3	C, CoreF(1910.8), 512(512.1)				
					7203 (C)	1020.3(2)	1018.138 (3)	1018.138	0	5	2	0	Man-5 [Figure 8, C1]				
					6895 (C)	1098.3(2)	1070.171 (3)	1070.172	0	5	2	0	Man-5				
					6165 (C)	1162.4(2)	1112.871 (3)	1112.870	0	5	2	0	Man-5				
					5086 (A, C)	1407.5	1211.037 (2)	1211.036	0	5	2	0	Man-5				
					— (B)	1407.7	883.729 (3)	883.730	1	3	4	0	CoreF(1553.5), bisectGN(1061.5)				
					—												
					—												
					8, D2	q-8 (2)											
					Q	SILTVTN <sup>249</sup> VTQE (1203.635)	17	8, D2	q-8 (2)	— (B)	1407.5	1211.037 (2)	1211.036	0	5	2	0
1407.7	883.729 (3)	883.730	1	3	4	0	CoreF(1553.5), bisectGN(1061.5)										

Table 1: Continued

protein	sequence <sup>a,b</sup>	glycopeptides					N-glycan						
		elution position	Figure	peak no. <sup>c</sup>	scan in Figure 4A <sup>d</sup>	observed peptide-related ion <sup>e</sup>	observed <i>m/z</i> in SIM mode <sup>b</sup>	theoretical <i>m/z</i> <sup>b</sup>	deduced monosaccharide composition				
									dHex	Hex	HexNAc	NA	
R HFGN <sup>257</sup> YTCVAANK (1380.624)	8, E2	10		q-10 (2)	5059 (A, C)	1407.4	1325.094 (2)	1325.092	1	3	4	0	CoreF(1553.5) or 512(512.2), bisectGN(988.6)
				— (B)	1407.6	951.423 (3)	951.423	1	3	5	0	C, CoreF(1553.6), bisectGN(988.6), BA-2	
				— (A)	1407.6	1426.632 (2)	1426.631	1	3	5	0	C, CoreF(1553.5), bisectGN(988.2), BA-2	
				q-11 (2)	4950 (A, C)	1407.5	1458.635 (2)	1458.634	2	5	3	0	H, CoreF(1553.4), 512(512.2)
				— (B)	1407.3	991.765 (3)	991.765	1	5	4	0	H, CoreF(1553.6)	
				— (A)	1407.6	1487.143 (2)	1487.144	1	5	4	0	H, CoreF(1553.4)	
				q-1	5126 (A)	1407.5	1021.106 (3)	1021.104	1	5	3	1	H, CoreF(1553.4) or 512(512.2)
				— (A)	1407.6	1531.153 (2)	1531.152	1	5	3	1	H, CoreF(1553.6) or 512(512.0)	
				q-2	4885 (C)	1407.4	1026.777 (3)	1026.776	2	6	3	0	H, CoreF(1553.5), L <sup>ax</sup> (350.3, 512.2)
				q-2 (2)	4919 (C)	1407.6	1539.663 (2)	1539.660	2	6	3	0	H, CoreF(1554.2), 512(512.1)
				q-3	5010 (A, C)	1407.5	1040.453 (3)	1040.451	2	5	4	0	H, CoreF(1553.6), L <sup>ax</sup> (350.2, 512.1)
				— (A)	1407.5	1560.174 (2)	1560.173	2	5	4	0	H, CoreF(1553.4), 512(512.2)	
				q-4	4944 (A, C)	1406.6	1054.128 (3)	1054.127	2	4	5	0	C, CoreF(1552.6)s, L <sup>ax</sup> (350.2, 512.1) [Figure 8, DI]
				— (A)	1407.6	1580.687 (2)	1580.687	2	4	5	0	C, CoreF(1553.6), 512(512.2)	
				— (A)	1407.5	1075.121(3)	1075.122	1	6	3	1	H, CoreF(1554.6)	
				— (A)	1407.6	1612.180 (2)	1612.179	1	6	3	1	H, CoreF(1554.5)	
				q-5	4827	1407.5	1089.139 (3)	1089.137	3	5	4	0	H, CoreF(1553.6), 512(512.1)
				— (A)	1407.5	1094.469 (3)	1094.469	2	6	4	0	H, CoreF(1554.3), L <sup>ax</sup> (350.3, 512.2)	
				— (A)	1407.3	1102.473 (3)	1102.473	1	4	5	1	C, CoreF(1552.7)	
				q-6	5032	1407.5	1137.486 (3)	1137.483	2	5	4	1	C, CoreF(1553.3), 512(512.2)
				q-7	4869 (A)	1407.6	1156.832 (3)	1156.830	3	5	5	0	C, CoreF(1553.5)
				— (A)	1407.6	1170.166 (3)	1170.166	1	4	6	1	C, CoreF(1553.3) or (sL <sup>ax</sup> (512.4, 803.6)	
				q-9	5054 (A)	1407.4	1272.870 (3)	1272.869	2	5	6	1	C, CoreF(1553.5) (sL <sup>ax</sup> (454.1, 512.2, 657.2, 803.2))
				— (B)	793.2(2)	866.690 (3)	866.690	0	5	2	0	Man-5	
				r-7 (2)	3214 (C)	1584.7	1299.536 (2)	1299.531	0	5	2	0	Man-5
				r-1	3339 (C)	1584.6	1010.422 (3)	1010.420	1	3	5	0	C, CoreF(1730.6), bisectGN(1077.0), BA-2
				r-2	3162 (A, C)	1584.7	1050.764 (3)	1050.762	1	5	4	0	H, CoreF(1730.5), bisectGN(1077.7) [Figure 8, E1]
				r-3	3139 (A, C)	1585.9	1085.774 (3)	1085.772	2	6	3	0	H, CoreF(1730.8), L <sup>ax</sup> (350.2, 512.2)

Table 1: Continued

peptides		glycopeptides					N-glycan						
protein	sequence <sup>a,b</sup>	elution position	Figure	peak no. <sup>c</sup>	scan in Figure 4A <sup>d</sup>	observed peptide-related ion <sup>e</sup>	observed <i>m/z</i> in SIM mode <sup>b</sup>	theoretical <i>m/z</i> <sup>b</sup>	deduced monosaccharide composition				deduced structure <sup>f</sup> (diagnostic ion)
									dHex	Hex	HexNAc	NA	
			r-4		3208 (C)	1585.7	1099.450 (3)	1099.448	2	5	4	0	H <sub>2</sub> CoreF(1731.7), L <sup>a/x</sup> (350.1, 512.1)
			r-5		3189	1584.7	1104.784 (3)	1104.780	1	6	4	0	H <sub>2</sub> CoreF(1730.6) or L <sup>a/x</sup> (350.4, 512.0)
			r-6		3144 (A)	1585.6	1113.127 (3)	1113.123	2	4	5	0	C <sub>2</sub> CoreF(1730.8), L <sup>a/x</sup> (350.1, 512.2)
					– (A)	1585.8	1134.118 (3)	1134.118	1	6	3	1	H <sub>2</sub> CoreF(1730.6) or 512(512.3)
					– (A)	1584.5	1153.466 (3)	1153.466	2	6	4	0	H <sub>2</sub> CoreF(1731.6), L <sup>a/x</sup> (350.1, 512.2)

<sup>a</sup> Theoretical peptide mass indicated in parentheses. <sup>b</sup> Monoisotopic values. <sup>c</sup> Peaks are numbered in decreasing order of their calculated mass. All glycopeptides are triply charged except for doubly charged ions indicated by (2) after the peak number. <sup>d</sup> Glycopeptides were characterized on the basis of alternative LC–MS<sup>n</sup> runs with conditions indicated in parentheses (A, a C30 column, scan range of *m/z* 1000–2000; B, a C30 column, scan range of *m/z* 700–2000; C, a C18 column, scan range of *m/z* 1000–2000). <sup>e</sup> Y<sub>1</sub><sup>n+</sup> or Y<sub>1α/β</sub><sup>n+</sup>, [(peptide + HexNAc + nH)/n]<sup>n+</sup>, or Y<sub>1α</sub><sup>n+</sup> · [(peptide + HexNAc + dHex + nH)/n]<sup>n+</sup>. All glycopeptide-related ions are singly charged except for doubly or triply charged ions indicated by (2) or (3). <sup>f</sup> Structures are deduced by MS<sup>n</sup>: C<sub>2</sub>, complex-type oligosaccharide; H<sub>2</sub>, hybrid-type oligosaccharide; Man-5-9, high mannose-type oligosaccharide containing 5–9 mannose residues; CoreF, trimannosylcore fucose; bisectGN, bisecting GlcNAc; diSia, disialic acid; L<sup>a/x</sup>, Lewis a/x structure; sL<sup>a/x</sup>, sialylated Lewis a/x structure; Asn – Asp conversion upon PNGase F digestion.

integrated mass spectrum (peaks f-1–9 and g-1–3 in panel F2 of Figure 5) and their MS/MS spectra suggested that complex-type oligosaccharides including Le<sup>a/x</sup> or Le<sup>b/y</sup> -modified and/or bisected oligosaccharides and BA-2 are attached to Asn272 (Table 1F).

(vii) *Asn287*. The MS/MS spectra of GPI-linked peptides were selected from all MS data on the basis of the GPI-characteristic oxonium ions, such as GlcN-Ino-PO<sub>4</sub><sup>+</sup> (*m/z* 422). The structures of the GPI moieties were characterized from their product ions appearing in the MS/MS spectra, and their peptide portions were identified by comparing their observed masses with the theoretical masses of predicted peptides. Figure 4B shows the TIC obtained by GCC-LC-MS<sup>n</sup> for the hydrophilic glycopeptides. On the basis of the presence of GPI-characteristic oxonium ions, the MS data of GPI-linked peptides were located at position 26. The 9.5% of spectra generated at elution position 26 were assigned to those of GPI-linked peptides of LAMP, OBCAM, and neurotrimin.

Figure 5G shows one of the MS/MS spectra acquired at position 26 (precursor ion,  $[M + 2H]^{2+}$  at  $m/z$  902.5; peak L2 in Figure 4C). On the basis of the GPI-characteristic oxonium ions, such as  $NH_2Et-PO_4-Man-GlcN^+$  ( $m/z$  447.2),  $NH_2Et-PO_4-(HexNAC-)Man-GlcN^+$  ( $m/z$  650.3),  $NH_2Et-PO_4-(HexNAC-)Man-GlcN-Ino-PO_4^+$  ( $m/z$  910.2),  $NH_2Et-PO_4-(HexNAC-)(Hex-)Man-GlcN-Ino-PO_4^+$  ( $m/z$  1072.2), and  $GlcN-Ino-PO_4^+$  ( $m/z$  422.2), this peptide was identified as the GPI-linked peptide. The product ion at  $m/z$  328.3 was assigned to  $GIN^{287}-NH-Et^+$  on the basis of the fragments that arose by successive cleavages of HexNAC ( $m/z$  1600.4), Ino- $PO_4$  ( $m/z$  1340.5), GlcN ( $m/z$  1178.3), Man- $PO_4-EtNH_2$  and Hex ( $m/z$  732.2), Hex ( $m/z$  570.2), and  $PO_4-Hex$  ( $m/z$  328.3). In addition, the product ions at  $m/z$  732.3 and 1072.2 suggested the existence of HexNAC-( $NH_2Et-PO_4-$ )(Hex)-Man3 in the core structure of GPI (inset of Figure 5G). The presence of a positional isomer was inferred from the acquisition of two different MS/MS spectra of GPI-linked peptides (precursor ion  $[M + 2H]^{2+}$ ,  $m/z$  903) at different elution times (Table 2). The alternative runs also suggested the presence of a Hex-Man1 and HexNAC-(Hex-)( $NH_2Et-PO_4-$ )Man3 (peak L1, data not shown, Table 2), and a nonsubstituted Man1 and HexNAC-( $NH_2Et-PO_4-$ )Man3 (data not shown, Table 2) in the GPI core structure.

**Glycosylation Analysis of OBCAM.** OBCAM has six potential N-glycosylation sites at Asn17, -43, -113, -258, -266, and -279, and the predicted linkage site of GPI is Asn295. From the peptide-related ions, peptides eluted at positions 2, 25, and 7 were estimated to be glycopeptides containing Asn17, -258, and -266, respectively (panels A1–C1 of Figure 6). Panels A2–C2 of Figure 6 show the integrated mass spectrum of glycopeptides obtained from positions 2, 25, and 7, respectively. The glycopeptide containing Asn43 is identical to VAWLN<sup>38</sup>R in LAMP. From the glycosylation at Asn38 in LAMP, Man-5-9 were inferred to be attached to Asn43 (panel A2 of Figure 5 and Table 1A). Although the MS/MS spectrum of the glycopeptide containing Asn113 (VHLIVQVPPQIMN<sup>113</sup>ISSD) was not acquired, glycosylation at Asn113 was corroborated by detection of VHLIVQVPPQIMD<sup>113</sup>ISSD after PNGase F treatment (data not shown). The feature of glycosylation at Asn279 was elucidated on the basis of the MS/MS spectra of glycosylated LGNTN<sup>279</sup>ASITLYGPGAVID which was



Table 2: Summary of GPI Structure in LAMP, OBCAM, and Neurotrimin

protein	peptide (theoretical MW <sup>b</sup> )	peak no. in Figure 4C	scan in Figure 4B	GPI-linked peptide				GPI moiety			
				observed peptide-related ion <sup>b</sup> (charge state)	observed <i>m/z</i> <sup>b</sup> (charge state)	calculated mass	core	deduced glycan composition			
								Man1	Hex	HexNAc	P-EtNH <sub>2</sub>
								Hex	Hex	Man3	theoretical MW <sup>b</sup>
LAMP	GIN <sup>287</sup> (302.3)	L1	3863	328.3 (1)	983.6 (2)	1965.1	1	1	1	1	1681.3
		L2	3828 <sup>c</sup> (Figure 5G)	328.3 (1)	902.5 (2)	1803.0	1	0	1	1	1519.2
			4040 <sup>c</sup>	328.3 (1)	903.1 (2)	1804.2	1	0	1	1	1519.2
OBCAM	GVN <sup>295</sup> (288.3)	O1	3701 (Figure 6D)	328.2 (1)	821.6 (2)	1641.1	1	0	0	1	1357.0
		O2	3701 (Figure 6D)	314.3 (1)	976.5 (2)	1951.0	1	1	1	1	1681.3
			3633 <sup>d</sup>	314.3 (1)	895.4 (2)	1788.7	1	0	1	1	1519.2
			3853 <sup>d</sup>	314.3 (1)	895.5 (2)	1788.9	1	0	1	1	1519.2
		O3	3805	314.3 (1)	814.6 (2)	1627.1	1	0	0	1	1357.0
neurotrimin	VNN <sup>289</sup> (345.4)	N1	3750	371.2 (1)	1004.8 (2)	2007.7	1	1	1	1	1681.3
		N2	3741 <sup>e</sup>	371.4 (1)	924.0 (2)	1846.1	1	0	1	1	1519.2
			3896 <sup>e</sup>	371.2 (1)	924.1 (2)	1846.1	1	0	1	1	1519.2
		N3	3873 (Figure 7D)	371.3 (1)	842.8 (2)	1683.5	1	0	0	1	1357.0

<sup>a</sup> The structure of GPI was deduced by another LC-MS<sup>n</sup> run. <sup>b</sup> Average value. <sup>c</sup> Isomers. <sup>d</sup> Isomers. <sup>e</sup> Isomers.

acquired in an alternative run with the C30 column (scan range of *m/z* 1000–2000) (Table 1J).

(i) *Asn 17*. As shown in panel A1 of Figure 6, the glycopeptide that eluted at position 2 was assigned to AMDN<sup>17</sup>VTVR (and/or AMDN<sup>12</sup>VTVR in neurotrimin) glycosylated with dHex<sub>1</sub>Hex<sub>5</sub>HexNAc<sub>4</sub>NeuAc<sub>4</sub> based on the Y<sub>1α</sub> ion and the monoisotopic mass of the molecular ion. The attachment of three NeuAc residues in one branch of a biantennary complex type was suggested by the existence of characteristic B ions (*m/z* 495.2, 744.9, and 1239.2) (panel A1 of Figure 6). The molecular ions appearing in the integrated mass spectrum and their MS/MS spectra suggested that most of the glycans at Asn17 were disialic acid-conjugated oligosaccharides (peaks h-1–3 in panel A2 of Figure 6 and Table 1G).

(ii) *Asn258*. Panel B1 of Figure 6 shows the representative MS/MS spectrum of glycosylated ISTLTFFN<sup>258</sup>VSE that eluted at position 25. The monosaccharide composition (dHex<sub>2</sub>Hex<sub>5</sub>HexNAc<sub>6</sub>NeuAc<sub>1</sub>) implied two possible structures: a sLe<sup>a/x</sup>-modified core-fucosylated complex type and a Le<sup>a/x</sup> or antigen H-modified core-fucosylated and sialylated complex type (inset of panel B1 of Figure 6). The molecular ions (peaks i-1–2) in the integrated mass spectrum (panel B2 of Figure 6) and the detection of nonglycosylated ISTLTFFN<sup>258</sup>VSE revealed that Asn258 is partly glycosylated with the sLe<sup>a/x</sup> or Le<sup>b/y</sup>-modified core-fucosylated complex type, and BA-2 (Table 1H).

(iii) *Asn266*. Panel C1 of Figure 6 shows the product ion spectra of the glycopeptide at position 7, the peptide portion of which was assigned to YGN<sup>266</sup>YTCVATNK on the basis of the Y<sub>1α/1β</sub> ion in the MS/MS/MS spectrum. The glycan was characterized as the bisected and core-fucosylated complex-type oligosaccharide containing Le<sup>a/x</sup> structure from the monosaccharide composition (dHex<sub>2</sub>Hex<sub>4</sub>HexNAc<sub>5</sub>), and the Le<sup>a/x</sup>-, bisecting-, and core-fucose-related ions. The MS/MS spectra acquired with other glycoforms (peaks j-1–4 in panel C2 of Figure 6) together with the MS/MS spectra of the glycopeptides DYGN<sup>266</sup>YTCVATNK (position 13) and KDYGN<sup>266</sup>YTCVATNK (position 6) suggested that the Le<sup>a/x</sup>-modified and/or bisected complex type and Man-5 were predominantly attached to Asn266 (Table 1I).

(iv) *Asn295*. On the basis of the GPI-characteristic oxonium ions and the peptide-related ion (*m/z* 314.3), the MS/MS spectrum of GPI-linked GVN<sup>295</sup> was picked out from position 26 (Figure 6D; precursor ion, *m/z* 976.5; peak O1 in Figure 4C). The fragments arising from the GPI moiety suggested the linkage of Hex to Man1, and HexNAc, Hex, and NH<sub>2</sub>Et-PO<sub>4</sub> to Man3 in the core structure (Figure 6D, inset). Furthermore, the MS/MS spectrum of other GPI-linked GVN<sup>295</sup> (precursor ion, *m/z* 895; peak O2), which was picked out from position 26 based on the peptide-related ion, suggested that this GPI moiety contained HexNAc-(Hex)-(NH<sub>2</sub>Et-PO<sub>4</sub>)Man3. Another MS/MS spectrum (precursor ion, *m/z* 814; peak O3) suggested the linkage of GPI moieties containing HexNAc-(NH<sub>2</sub>Et-PO<sub>4</sub>)Man3 (Table 2). The existence of two isomers was suggested in peak O2 by the acquisition of two MS/MS spectra of GPI-GVN<sup>295</sup> (*m/z* 895) at different elution times.

*Glycosylation Analysis of Neurotrimin*. Neurotrimin contains seven potential N-glycosylation sites at Asn12, -38, -120, -184, -252, -260, and -273, and the predicted linkage site of GPI is Asn289. As the amino acid sequence in the

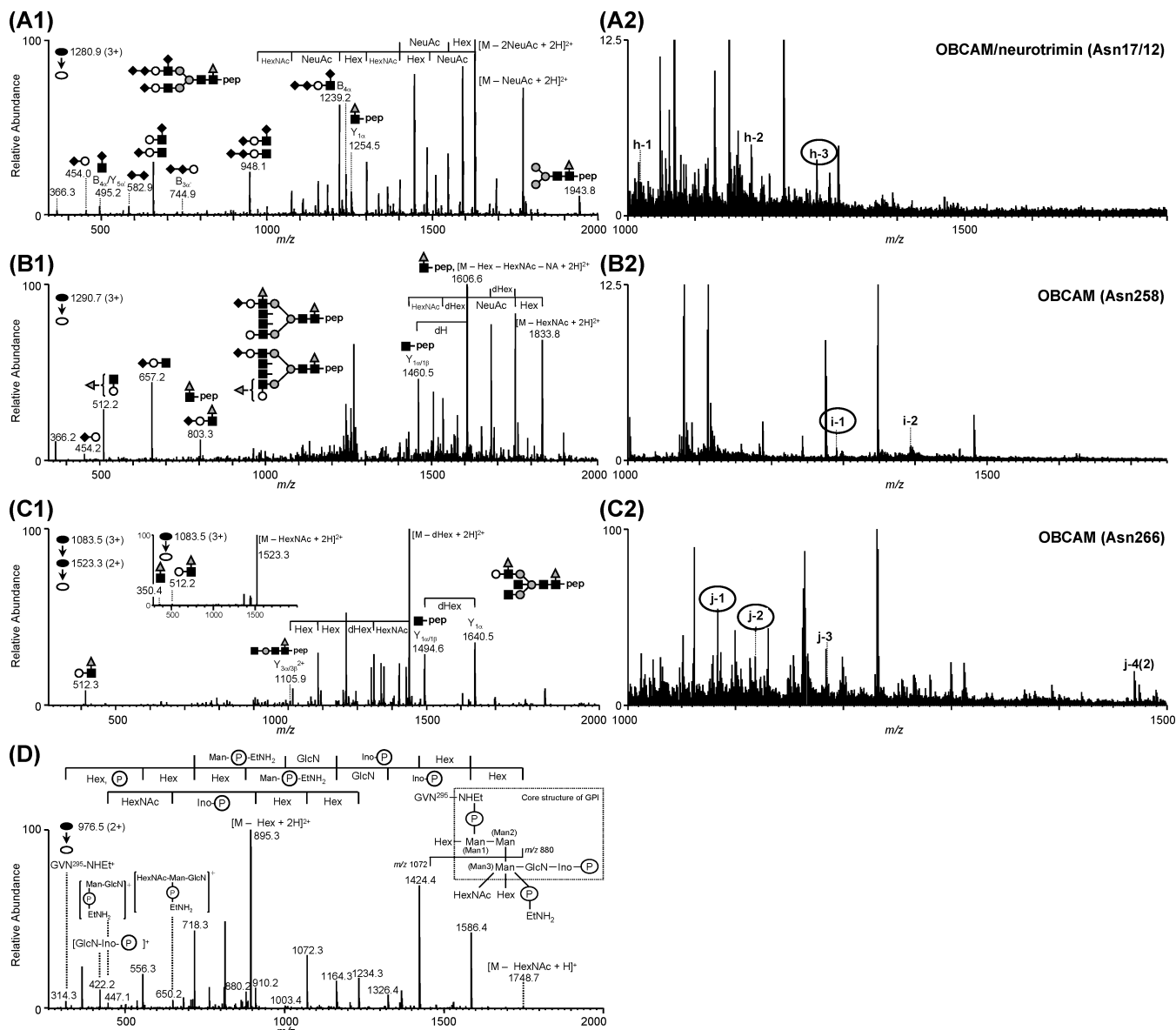


FIGURE 6: MS spectra of OBCAM glycopeptides. (A1) MS/MS spectra of glycopeptide AMDN<sup>17</sup>VTVR; elution position, 2; precursor ion,  $[M + 3H]^{3+}$  ( $m/z$  1280.9). (A2) Integrated mass spectrum obtained from position 2. (B1) MS/MS spectrum of glycopeptide ISTLTFFN<sup>258</sup>VSE; elution position, 25; precursor ion,  $[M + 3H]^{3+}$  ( $m/z$  1290.7). (B2) Integrated mass spectrum at position 25. (C1) MS/MS and MS/MS/MS spectra of glycopeptide YGN<sup>266</sup>YTCVATNK; elution position, 7; precursor ion,  $[M + 3H]^{3+}$  ( $m/z$  1083.5). (C2) Integrated mass spectrum at position 7. (D) MS/MS spectrum of GPI-linked GVN<sup>295</sup>; elution position, 26; precursor ion,  $[M + 2H]^{2+}$  ( $m/z$  976.5). Symbols are as in Figure 9.

glycopeptide containing Asn12 (GTDN<sup>12</sup>ITVR) in neurotrimin is identical to GTDN<sup>17</sup>ITVR in OBCAM, the glycans at Asn12 are estimated to be hybrid and complex types containing disialic acid (panel A2 of Figure 6 and Table 1G). Likewise, the sequence of VAWLN<sup>38</sup>R in neurotrimin is identical to that of VAWLN<sup>38</sup>R in LAMP, and therefore, the linkage of Man-5-9 at Asn38 was inferred from the glycosylation at Asn38 in LAMP (panel A2 of Figure 5 and Table 1A). Although the MS/MS spectra of glycopeptides containing Asn120 were not acquired, glycosylation at Asn120 was confirmed by the identification of GND<sup>120</sup>ISLTCIATGR, GND<sup>120</sup>ISLTCIATGRPE, and GND<sup>120</sup>ISLTCIATGRPEPTVTWR after PNGase F digestion (data not shown). The substitution of Asn184 with a Lys or an Arg residue in neurotrimin was suggested as in case of SD rat by the identification of VTVNYPPYISE, which is a fragment of VN<sup>184</sup>VTVNYPPYISE (data not shown) (33).

The MS/MS spectra of glycopeptides containing Asn252, -260, -273, and -289 were located at positions 20, 5, 23, and 26 based on the peptide-related ions, respectively (panels A1–C1 and D of Figure 7). The integrated mass spectrum of the glycopeptides containing Asn252, -260, and -273 are shown in panels A2–C2 of Figure 7, respectively.

(i) *Asn252*. Panel A1 of Figure 7 shows the representative MS/MS spectra of glycopeptide LTFFN<sup>252</sup>VSE linked by dHex<sub>2</sub>Hex<sub>6</sub>HexNac<sub>4</sub>, acquired at position 20. A Le<sup>a/x</sup>-modified core-fucosylated and bisected hybrid-type oligosaccharide was deduced from the Le<sup>a/x</sup>-related ions, and Y<sub>1β/3α/3β</sub><sup>2+</sup> and Y<sub>1α</sub>. The majority of the glycans at Asn252 are estimated to be Le<sup>a/x</sup> or Le<sup>b/y</sup>-modified complex- and hybrid-type oligosaccharides from the molecular ions (peaks k-1–9) in the integrated mass spectrum and their MS/MS spectra (panel A2 of Figure 7 and Table 1K).

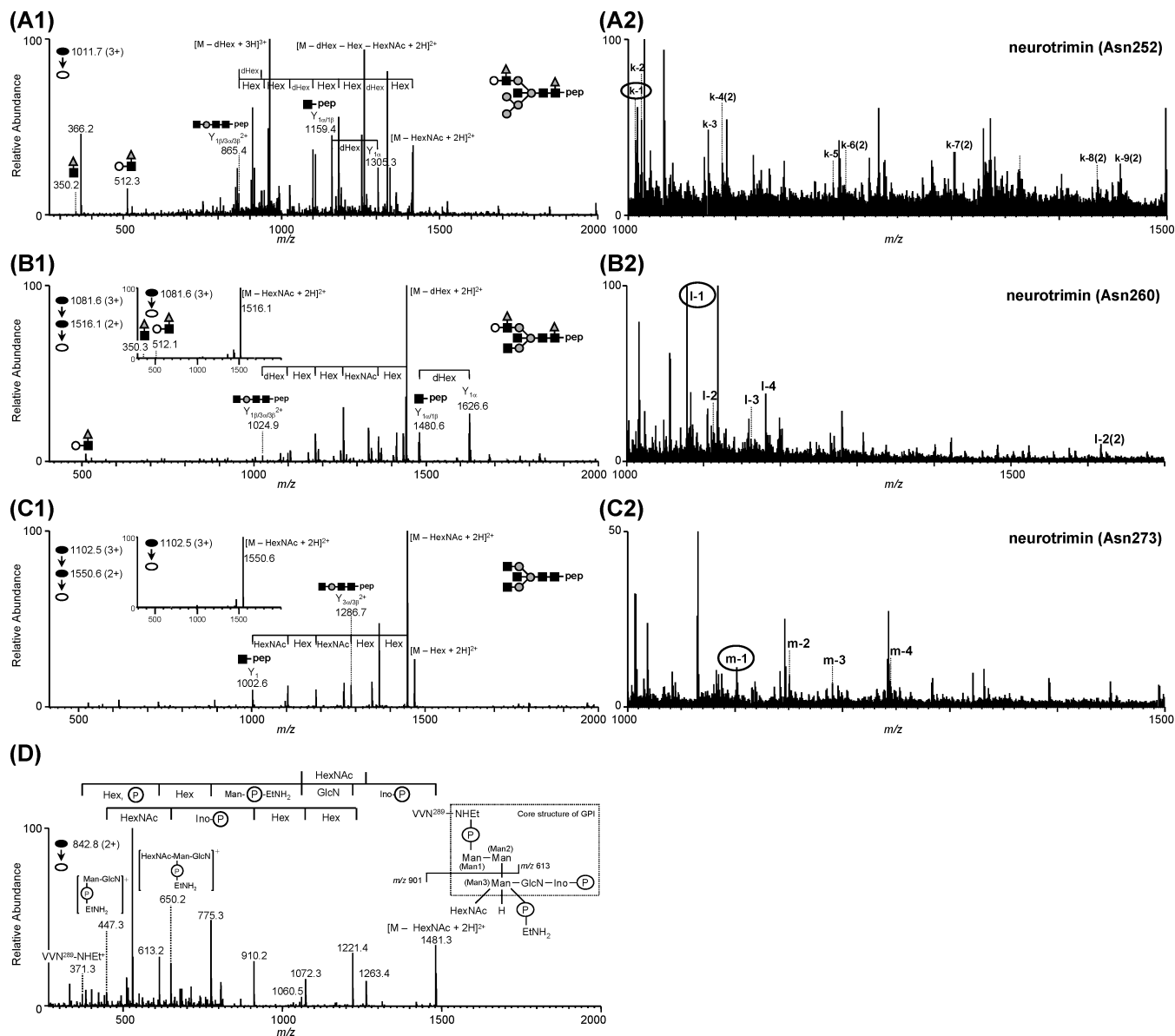


FIGURE 7: MS spectra of neurotrimin glycopeptides. (A1) MS/MS spectra of glycopeptide LTFN<sup>252</sup>VSE; elution position, 20; precursor ion,  $[M + 3H]^{3+}$  ( $m/z$  1011.7). (A2) Integrated mass spectrum obtained from position 20. (B1) MS/MS and MS/MS/MS spectra of glycopeptide YGN<sup>260</sup>YTCVASNK; elution position, 5; precursor ion,  $[M + 3H]^{3+}$  ( $m/z$  1081.6). (B2) Integrated mass spectrum at position 5. (C1) MS/MS and MS/MS/MS spectra of glycopeptide LGHTN<sup>273</sup>ASIMLFPGAVSE; elution position, 23; precursor ion,  $[M + 3H]^{3+}$  ( $m/z$  1102.5). (C2) Integrated mass spectrum at position 23. (D) MS/MS spectrum of GPI-linked VNN<sup>289</sup>; elution position, 26; precursor ion,  $[M + 2H]^{2+}$  ( $m/z$  842.8). Symbols are as in Figure 9.

(ii) *Asn260*. Panel B1 of Figure 7 shows the representative product ion spectra of the glycopeptide eluted at position 5, the peptide portion of which was identified as YGN<sup>260</sup>YTCVASNK on the basis of the  $Y_{1\alpha/1\beta}$  ion in the MS/MS/MS spectrum. The monosaccharide composition (dHex<sub>2</sub>Hex<sub>4</sub>HexNAc<sub>5</sub>), the Le<sup>a/x</sup>-related ions in the MS/MS spectrum, and the presence of  $Y_{1\beta/3\alpha/3\beta}^{2+}$  and  $Y_{1\alpha}$  in the MS/MS/MS spectrum revealed the linkage of a Le<sup>a/x</sup>-modified fucosylated and bisected complex-type oligosaccharide to this peptide (inset of panel B1 of Figure 7). The molecular ions in the integrated mass spectrum (peaks l-1–4 in panel B2 of Figure 7) together with the MS/MS spectra of glycosylated HDYGN<sup>260</sup>YTCVASNK (position 8) suggested that Asn260 was predominantly glycosylated with the Le<sup>a/x</sup> or Le<sup>b/y</sup>-modified bisected complex- and hybrid-type oligosaccharides and BA-2 (Table 1L).

(iii) *Asn273*. On the basis of the  $Y_1$  ion and the monoisotopic mass, the glycopeptide eluted at position 23 was assigned to LGHTN<sup>273</sup>ASIMLFPGAVSE glycosylated with Hex<sub>3</sub>HexNAc<sub>5</sub> (panel C1 of Figure 7). Its glycan moiety was characterized as a bisected agalacto-complex-type oligosaccharide based on  $Y_{3\alpha/3\beta}^{2+}$ . Other glycans at Asn273 were assigned to bisected complex- and hybrid-type oligosaccharides (peaks m-1–4 in panel C2 of Figure 7 and Table 1M).

(iv) *Asn289*. Figure 7D shows one of the MS/MS spectra of GPI-linked VNN<sup>289</sup>, which was picked out from position 26 on the basis of the peptide-related ion (peptide-NH-Et<sup>+</sup>,  $m/z$  371.3). Three different MS/MS spectra of GPI-linked VNN<sup>289</sup> were picked out from position 26 (Figure 4B). From the molecular ions [peaks N1 ( $m/z$  1004), N2 ( $m/z$  924), and N3 ( $m/z$  842)] and their fragments, it was suggested that they contain Hex-Man1 and HexNAc-(Hex-)(NH<sub>2</sub>Et-PO<sub>4</sub>-)Man<sub>3</sub>,

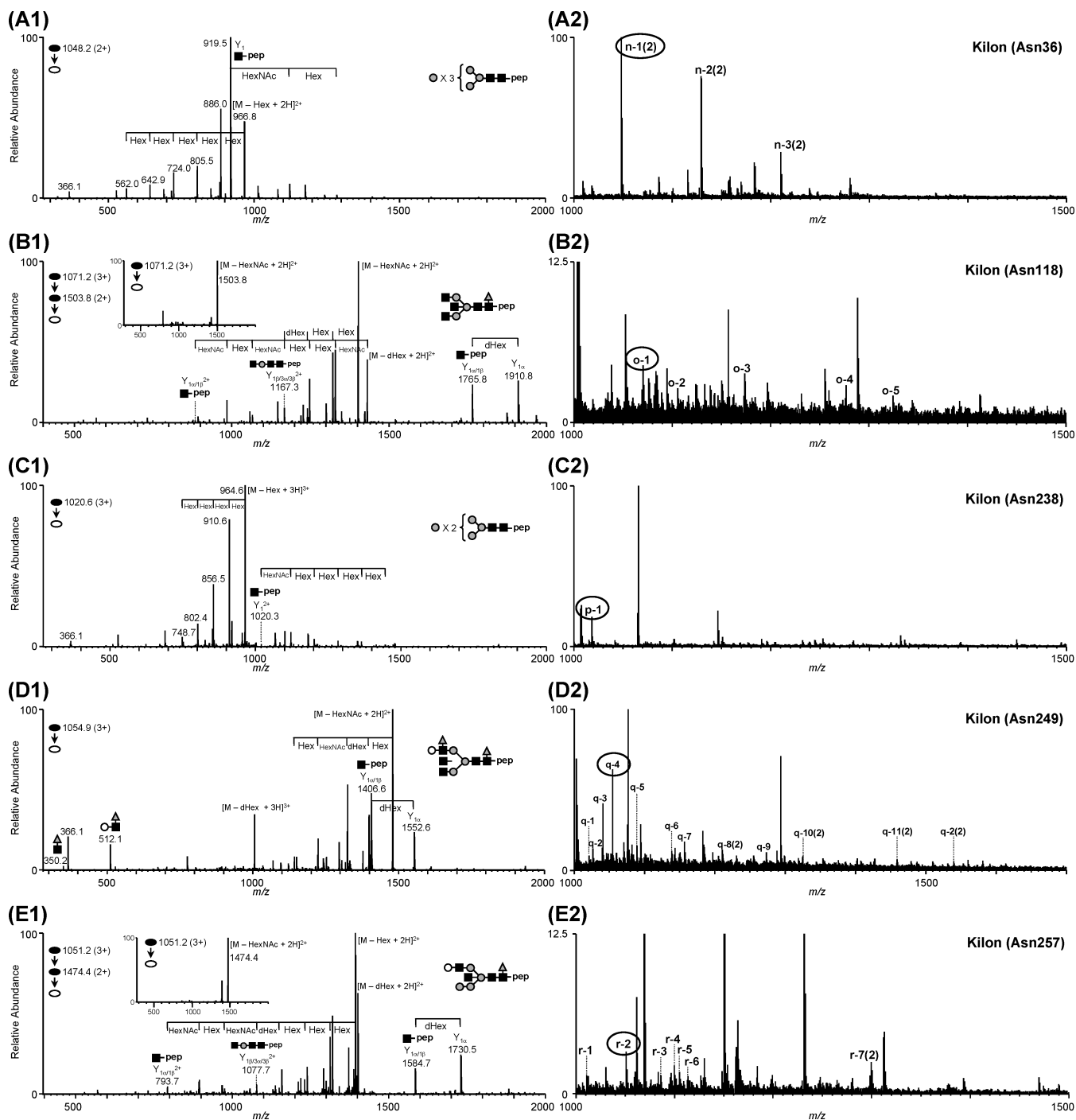


FIGURE 8: MS spectra of Kilon glycopeptides. (A1) MS/MS spectra of glycopeptide GAWLN<sup>36</sup>R; elution position, 3; precursor ion,  $[M + 2H]^{2+}$  ( $m/z$  1048.2). (A2) Integrated mass spectrum obtained from position 3. (B1) MS/MS and MS/MS/MS spectra of glycopeptide GTN<sup>118</sup>VTLTCLATGKPE; elution position, 16; precursor ion,  $[M + 3H]^{3+}$  ( $m/z$  1071.2). (B2) Integrated mass spectrum at position 16. (C1) MS/MS spectrum of glycopeptide LFNGQQGIIIQN<sup>238</sup>FSTR; elution position, 22; precursor ion,  $[M + 3H]^{3+}$  ( $m/z$  1020.6). (C2) Integrated mass spectrum at position 22. (D1) MS/MS spectrum of glycopeptide SILTVTN<sup>249</sup>VTQE; elution position, 17; precursor ion,  $[M + 3H]^{3+}$  ( $m/z$  1054.9). (D2) Integrated mass spectrum at position 17. (E1) MS/MS and MS/MS/MS spectra of glycopeptide HFGN<sup>257</sup>YTCVAANK; elution position, 10; precursor ion,  $[M + 3H]^{3+}$  ( $m/z$  1051.2). (E2) Integrated mass spectrum at position 10. Symbols are as in Figure 9.

HexNAc-(Hex-)(NH<sub>2</sub>Et-PO<sub>4</sub>-)Man<sub>3</sub>, and HexNAc-(NH<sub>2</sub>Et-PO<sub>4</sub>-)Man<sub>3</sub>, respectively. The existence of two isomers was suggested in peak N2 by the presence of two different MS/MS spectra at different elution times (Table 2).

**Glycosylation Analysis of Kilon.** Kilon has six potential N-glycosylation sites at Asn36, -118, -238, -249, -257, and -270. The predicted linkage site of GPI is Gly287. The typical MS/MS spectra and the integrated mass spectra of the glycopeptides containing Asn36, -118, -238, -249, and -257

are shown in panels A1–E1 and A2–E2 of Figure 8, respectively. The MS/MS spectra of the glycopeptide containing both Asn270 and Gly287 could not be picked out from the MS data.

(i) *Asn36.* Panel A1 of Figure 8 shows one of the MS/MS spectra acquired at position 3. This glycopeptide was identified as GAWLN<sup>36</sup>R with Man-6 based on Y<sub>1</sub> ion and the monosaccharide composition. Other glycans at Asn36 were estimated as Man-5, -7, and -8 from the existence of



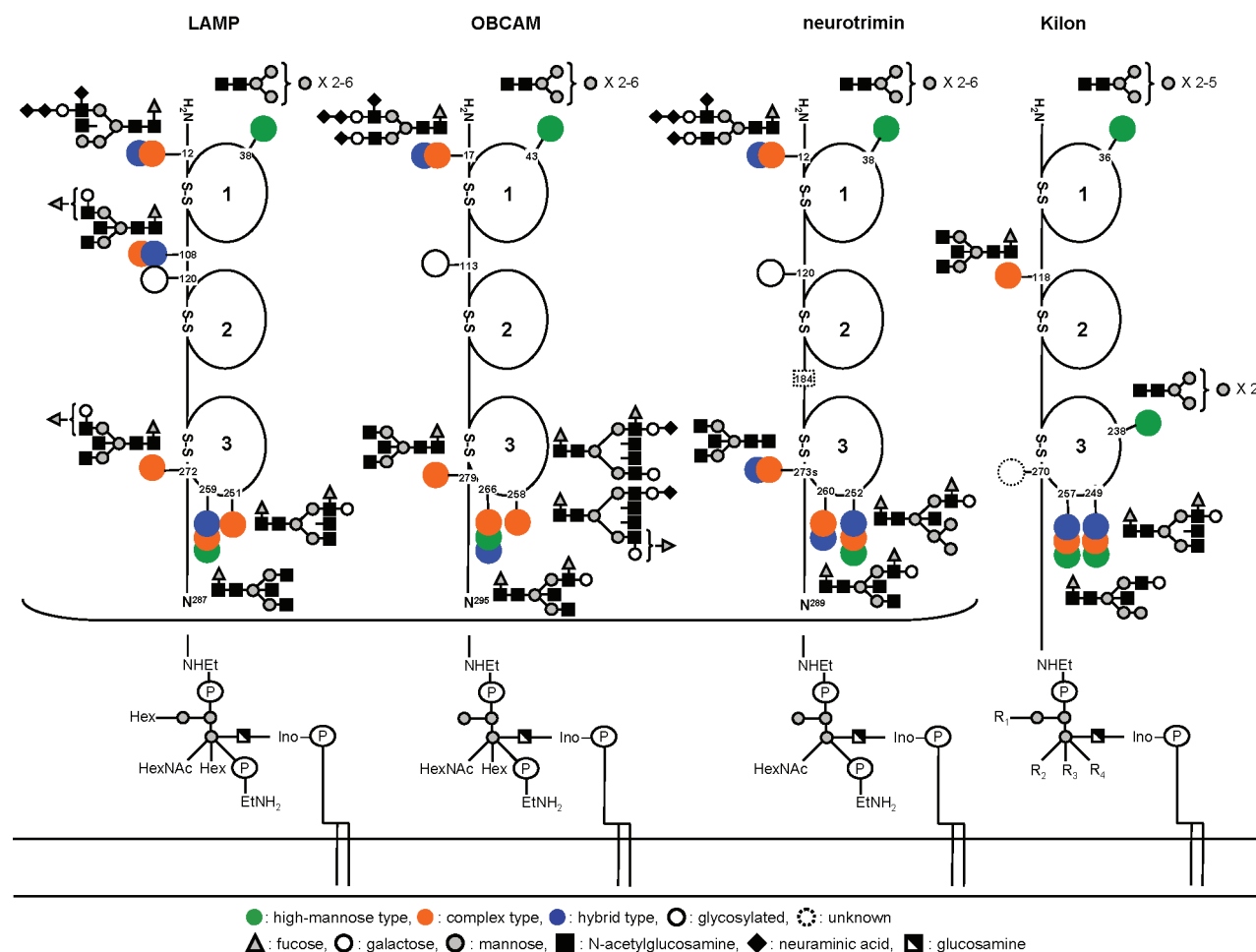


FIGURE 9: Summary of glycosylation of IgLON family proteins.

molecular ions with 81  $m/z$  units intervals in the integrated mass spectrum (peaks n-1–3 in panel A2 of Figure 8) (Table 1N).

(ii) *Asn118*. As shown in panel B1 of Figure 8, the MS/MS spectrum acquired at position 16 contained  $Y_{1\alpha/1\beta}$ , which suggested that the peptide portion is GTN<sup>118</sup>VTLTCLATGKPE. The linkage of BA-2 was deduced from the monosaccharide composition (dHex<sub>1</sub>Hex<sub>3</sub>HexNAc<sub>5</sub>), and  $Y_{1\beta/3\alpha/3\beta}^{2+}$  and  $Y_{1\alpha}$  (inset of panel B1 of Figure 8). Additionally, the linkage of Le<sup>a/x</sup> or antigen H-modified and/or bisected complex type was suggested by the integrated mass spectrum (peaks o-1–5 in panel B2 of Figure 8 and Table 1O).

(iii) *Asn238*. The MS/MS spectra of glycopeptides that contain Asn238 were picked out from positions 22 [LFNGQQGIIIQN<sup>238</sup>FSTR (panel C1 of Figure 8)], 21 (RLFNGQQGIIIQN<sup>238</sup>FSTR), and 19 (KRLFNGQQGIIIQN<sup>238</sup>FSTR). These MS/MS spectra and molecular ions appearing in the integrated mass spectrum revealed that the only carbohydrate structure at Asn238 was Man-5 (peak p-1 in panel C2 of Figure 8 and Table 1P). Together with the results of the database search analysis, in which nonglycosylated peptide LFNGQQGIIIQN<sup>238</sup>FSTR was identified, it was suggested that Man-5 was partly attached to Asn238 (Table 1P).

(iv) *Asn249*. Panel D1 of Figure 8 shows the representative MS/MS spectrum of glycopeptide SILTVTN<sup>249</sup>VTQE at position 17. The carbohydrate structure was characterized as a Le<sup>a/x</sup>-modified and core-fucosylated complex type by

the existence of the Le<sup>a/x</sup>-related ions and  $Y_{1\alpha}$ . The integrated mass spectrum and alternative LC–MS<sup>n</sup> with the C30 column (scan ranges of  $m/z$  700–2000 and 1000–2000) suggested that Asn249 is glycosylated with Le<sup>a/x</sup> or antigen H-modified core-fucosylated hybrid- and complex-type oligosaccharides, BA-2, and Man-5 (peaks q-1–11 in panel D2 of Figure 8 and Table 1Q).

(v) *Asn257*. As shown in panel E1 of Figure 8, one of the glycopeptides eluted at position 10 was identified as HFGN<sup>257</sup>YTCVAANK linked by dHex<sub>1</sub>Hex<sub>5</sub>HexNAc<sub>4</sub> based on  $Y_{1\alpha/1\beta}$  ion in the MS/MS/MS spectra and monoisotopic mass. The carbohydrate structure was characterized as a bisected- and core-fucosylated hybrid-type oligosaccharide based on the presence of  $Y_{1\beta/3\alpha/3\beta}^{2+}$  and  $Y_{1\alpha}$  (inset of panel E2 of Figure 8). Other major glycans were estimated as Man-5, Le<sup>a/x</sup>-modified complex- and hybrid-type oligosaccharides, and BA-2 (peaks r-1–7 in panel E2 of Figure 8 and Table 1R).

## DISCUSSION

The cell adhesion molecules in the central nervous system play an essential role in the differentiation of neuronal cells and formation of neural circuits. Although glycosylation on the cell adhesion molecules is known to regulate cell–cell interactions (2–4), their carbohydrate structures remain unknown due to the difficulty with respect to their isolation and the limited sample amounts. The glycans in the IgLON family proteins are considered to be implicated in the

formation of neural circuits, including migration of neuronal cells, axonal guidance, and fasciculation. However, the high degree of homology of their amino acid sequences makes it difficult to isolate them from each other and to analyze their carbohydrate structures in detail.

In this study, we performed a site-specific glycosylation analysis of LAMP, OBCAM, neurotrimin, and Kilon simultaneously using SDS-PAGE and LC-MS<sup>n</sup>. Enriched GPI-linked proteins were separated by SDS-PAGE, and four target proteins were extracted from a gel piece together with other contaminating proteins. The protein mixture was digested and analyzed by the C30 and C18-LC-MS<sup>n</sup> runs via MS, data-dependent MS in SIM by the FT ICR-MS, and data-dependent MS/MS and MS/MS/MS. A set of MS data consisting of the mass spectrum, the mass spectrum acquired by the FT ICR-MS in SIM mode, the data-dependently acquired MS/MS, and the MS/MS/MS spectra of a glycopeptide was selected from all MS data on the basis of the existence of the oligosaccharide characteristic oxonium ions in the MS/MS spectrum. The carbohydrate structure and peptide sequence were deduced from the carbohydrate-related ions and peptide-related ions in the product ion spectra. The structural assignment of the glycopeptide was confirmed by the accurate mass acquired on the FT ICR-MS. The b- and y-ions arising from the peptide backbone in the MS/MS/MS spectra were also used for the peptide assignment. The carbohydrate heterogeneity at each glycosylation site was characterized by integrating the mass spectra of the glycopeptides which yielded identical peptide-related ions. We successfully determined the site-specific glycosylation in LAMP, OBCAM, neurotrimin, and Kilon with the exception of Asn120 in LAMP, Asn113 in OBCAM, Asn120 in neurotrimin, and Asn270 in Kilon. We also demonstrated the structure of the GPI moiety using LC-MS<sup>n</sup> equipped with a GCC. A set of data was picked out from all MS data by using GPI-characteristic ions, and the structure of GPI and the linkage site were deduced from the product ions in the MS/MS spectra. Three different structures are commonly found in LAMP, OBCAM, and neurotrimin.

Figure 9 illustrates the site-specific glycosylation in the four proteins. N-Glycosylation sites near the N-terminus in LAMP, OBCAM, and neurotrimin were commonly occupied with biantennary complex-type and hybrid-type oligosaccharides containing disialic acids. Oligosialic acids and disialic acids, which are found in several glycoproteins, including NCAM, are considered to regulate the cell-cell interaction by changing their degree of polymerization (6). Disialic acids at the near N-terminus in LAMP, OBCAM, and neurotrimin might regulate the cell-cell interaction in a manner similar to that of other glycosylated adhesion molecules.

The first domains in IgLON family proteins are commonly glycosylated with Man-5, -6, -7, -8, and -9. The linkage of high-mannose-type oligosaccharides is found in several Ig superfamily proteins, including L1, MAG, and P0 (3). Since Horstkorte et al. have reported that L1 binds to NCAM through oligomannosidic carbohydrates in L1 (34), the high-mannose-type oligosaccharide in IgLON family proteins could interact with certain biological molecules.

The third domains of all IgLON proteins were highly heterogeneous due to a linkage of diverse oligosaccharides, including BA-2, the Le<sup>a/x</sup> or Le<sup>b/y</sup> motif, and Man-5. BA-2,

a bisected agalacto-complex type, is known as a brain-specific glycan and is much more abundant in mammalian brains than in other tissues (35, 36). Recently, the Na<sup>+</sup>/K<sup>+</sup>-ATPase  $\beta$ 1 subunit was identified as a GlcNAc-binding protein in the mouse brain (37). The Na<sup>+</sup>/K<sup>+</sup>-ATPase  $\beta$ 1 subunit is a potassium-dependent lectin which binds to GlcNAc-terminating oligosaccharides and is involved in neural cell interactions in a trans-binding fashion. A 74 kDa protein was suggested to be the GlcNAc-terminating glycan carrier protein binding to the Na<sup>+</sup>/K<sup>+</sup>-ATPase  $\beta$ 1 subunit. The linkage of BA-2 to IgLON family proteins implies that these proteins might be the ligand proteins for the Na<sup>+</sup>/K<sup>+</sup>-ATPase  $\beta$ 1 subunit.

Glycosylation in a great number of membrane glycoproteins remains largely unknown. This is mainly because the limited amount of available sample and the low solubility of glycoproteins make their isolation quite difficult. Our strategy, which includes enrichment of the target glycoproteins, separation by SDS-PAGE, and LC-MS<sup>n</sup> of digests of a protein mixture, can be applied to the site-specific glycosylation analysis of various membrane glycoproteins.

## ACKNOWLEDGMENT

We thank Dr. Masayuki Kubota and Morihiko Yoshida (Thermo Fisher Scientific K.K.) for their technical support.

## REFERENCES

- Walsh, F. S., and Doherty, P. (1997) Neural cell adhesion molecules of the immunoglobulin superfamily: Role in axon growth and guidance. *Annu. Rev. Cell Dev. Biol.* 13, 425-456.
- Kleene, R., and Schachner, M. (2004) Glycans and neural cell interactions. *Nat. Rev. Neurosci.* 5, 195-208.
- Krog, L., and Bock, E. (1992) Glycosylation of neural cell adhesion molecules of the immunoglobulin superfamily. *APMIS, Suppl.* 27, 53-70.
- Schachner, M., and Martini, R. (1995) Glycans and the modulation of neural-recognition molecule function. *Trends Neurosci.* 18, 183-191.
- Liedtke, S., Geyer, H., Wuhler, M., Geyer, R., Frank, G., Gerardy-Schahn, R., Zahringer, U., and Schachner, M. (2001) Characterization of N-glycans from mouse brain neural cell adhesion molecule. *Glycobiology* 11, 373-384.
- Rutishauser, U. (1996) Polysialic acid and the regulation of cell interactions. *Curr. Opin. Cell Biol.* 8, 679-684.
- Kunemund, V., Jungalwala, F. B., Fischer, G., Chou, D. K., Keilhauer, G., and Schachner, M. (1988) The L2/HNK-1 carbohydrate of neural cell adhesion molecules is involved in cell interactions. *J. Cell Biol.* 106, 213-223.
- Cho, T. M., Hasegawa, J., Ge, B. L., and Loh, H. H. (1986) Purification to apparent homogeneity of a  $\mu$ -type opioid receptor from rat brain. *Proc. Natl. Acad. Sci. U.S.A.* 83, 4138-4142.
- Funatsu, N., Miyata, S., Kumanogoh, H., Shigeta, M., Hamada, K., Endo, Y., Sokawa, Y., and Maekawa, S. (1999) Characterization of a novel rat brain glycosylphosphatidylinositol-anchored protein (Kilon), a member of the IgLON cell adhesion molecule family. *J. Biol. Chem.* 274, 8224-8230.
- Levitt, P. (1984) A monoclonal antibody to limbic system neurons. *Science* 223, 299-301.
- Pimenta, A. F., Zhukareva, V., Barbe, M. F., Reinoso, B. S., Grimley, C., Henzel, W., Fischer, I., and Levitt, P. (1995) The limbic system-associated membrane protein is an Ig superfamily member that mediates selective neuronal growth and axon targeting. *Neuron* 15, 287-297.
- Schofield, P. R., McFarland, K. C., Hayflick, J. S., Wilcox, J. N., Cho, T. M., Roy, S., Lee, N. M., Loh, H. H., and Seeburg, P. H. (1989) Molecular characterization of a new immunoglobulin superfamily protein with potential roles in opioid binding and cell contact. *EMBO J.* 8, 489-495.
- Struyk, A. F., Canoll, P. D., Wolfgang, M. J., Rosen, C. L., D'Eustachio, P., and Salzer, J. L. (1995) Cloning of neurotrimin

- defines a new subfamily of differentially expressed neural cell adhesion molecules. *J. Neurosci.* 15, 2141–2156.
14. Brauer, A. U., Savaskan, N. E., Plaschke, M., Prehn, S., Ninnemann, O., and Nitsch, R. (2000) IG-molecule Kilon shows differential expression pattern from LAMP in the developing and adult rat hippocampus. *Hippocampus* 10, 632–644.
  15. Gil, O. D., Zhang, L., Chen, S., Ren, Y. Q., Pimenta, A., Zanazzi, G., Hillman, D., Levitt, P., and Salzer, J. L. (2002) Complementary expression and heterophilic interactions between IgLON family members neurotrimin and LAMP. *J. Neurobiol.* 51, 190–204.
  16. Hachisuka, A., Nakajima, O., Yamazaki, T., and Sawada, J. (2000) Developmental expression of opioid-binding cell adhesion molecule (OBCAM) in rat brain. *Brain Res. Dev. Brain Res.* 122, 183–191.
  17. Miyata, S., Matsumoto, N., Taguchi, K., Akagi, A., Iino, T., Funatsu, N., and Maekawa, S. (2003) Biochemical and ultrastructural analyses of IgLON cell adhesion molecules, Kilon and OBCAM in the rat brain. *Neuroscience* 117, 645–658.
  18. Zacco, A., Cooper, V., Chantler, P. D., Fisher-Hyland, S., Horton, H. L., and Levitt, P. (1990) Isolation, biochemical characterization and ultrastructural analysis of the limbic system-associated membrane protein (LAMP), a protein expressed by neurons comprising functional neural circuits. *J. Neurosci.* 10, 73–90.
  19. Hachisuka, A., Yamazaki, T., Sawada, J., and Terao, T. (1996) Characterization and tissue distribution of opioid-binding cell adhesion molecule (OBCAM) using monoclonal antibodies. *Neurochem. Int.* 28, 373–379.
  20. Wada, Y., Tajiri, M., and Yoshida, S. (2004) Hydrophilic affinity isolation and MALDI multiple-stage tandem mass spectrometry of glycopeptides for glycoproteomics. *Anal. Chem.* 76, 6560–6565.
  21. Wührer, M., Hokke, C. H., and Deelder, A. M. (2004) Glycopeptide analysis by matrix-assisted laser desorption/ionization tandem time-of-flight mass spectrometry reveals novel features of horseradish peroxidase glycosylation. *Rapid Commun. Mass Spectrom.* 18, 1741–1748.
  22. Satomi, Y., Shimonishi, Y., and Takao, T. (2004) N-Glycosylation at Asn(491) in the Asn-Xaa-Cys motif of human transferrin. *FEBS Lett.* 576, 51–56.
  23. Zaia, J. (2004) Mass spectrometry of oligosaccharides. *Mass Spectrom. Rev.* 23, 161–227.
  24. Wührer, M., Catalina, M. I., Deelder, A. M., and Hokke, C. H. (2007) Glycoproteomics based on tandem mass spectrometry of glycopeptides. *J. Chromatogr., B: Anal. Technol. Biomed. Life Sci.* 849, 115–128.
  25. Wührer, M., Koeleman, C. A., Hokke, C. H., and Deelder, A. M. (2005) Protein glycosylation analyzed by normal-phase nano-liquid chromatography-mass spectrometry of glycopeptides. *Anal. Chem.* 77, 886–894.
  26. Harazono, A., Kawasaki, N., Kawanishi, T., and Hayakawa, T. (2005) Site-specific glycosylation analysis of human apolipoprotein B100 using LC/ESI MS/MS. *Glycobiology* 15, 447–462.
  27. Sandra, K., Devreese, B., Van Beeumen, J., Stals, I., and Claeysens, M. (2004) The Q-Trap mass spectrometer, a novel tool in the study of protein glycosylation. *J. Am. Soc. Mass Spectrom.* 15, 413–423.
  28. Itoh, S., Kawasaki, N., Harazono, A., Hashii, N., Matsuishi, Y., Kawanishi, T., and Hayakawa, T. (2005) Characterization of a gel-separated unknown glycoprotein by liquid chromatography/multistage tandem mass spectrometry: Analysis of rat brain Thy-1 separated by sodium dodecyl sulfate-polyacrylamide gel electrophoresis. *J. Chromatogr., A* 1094, 105–117.
  29. Bordier, C. (1981) Phase separation of integral membrane proteins in Triton X-114 solution. *J. Biol. Chem.* 256, 1604–1607.
  30. Lisanti, M. P., Sargiacomo, M., Graeve, L., Saltiel, A. R., and Rodriguez-Boulant, E. (1988) Polarized apical distribution of glycosyl-phosphatidylinositol-anchored proteins in a renal epithelial cell line. *Proc. Natl. Acad. Sci. U.S.A.* 85, 9557–9561.
  31. Itoh, S., Kawasaki, N., Ohta, M., and Hayakawa, T. (2002) Structural analysis of a glycoprotein by liquid chromatography-mass spectrometry and liquid chromatography with tandem mass spectrometry. Application to recombinant human thrombomodulin. *J. Chromatogr., A* 978, 141–152.
  32. Kikuchi, M., Hatano, N., Yokota, S., Shimozaawa, N., Imanaka, T., and Taniguchi, H. (2004) Proteomic analysis of rat liver peroxisome: Presence of peroxisome-specific isozyme of Lon protease. *J. Biol. Chem.* 279, 421–428.
  33. Nakajima, O., Hachisuka, A., Takagi, K., Yamazaki, T., Ikebuchi, H., and Sawada, J. (1997) Expression of opioid-binding cell adhesion molecule (OBCAM) and neurotrimin (NTM) in *E. coli* and their reactivity with monoclonal anti-OBCAM antibody. *NeuroReport* 8, 3005–3008.
  34. Horstkorte, R., Schachner, M., Magyar, J. P., Vorherr, T., and Schmitz, B. (1993) The fourth immunoglobulin-like domain of NCAM contains a carbohydrate recognition domain for oligomannosidic glycans implicated in association with L1 and neurite outgrowth. *J. Cell Biol.* 121, 1409–1421.
  35. Chen, Y. J., Wing, D. R., Guile, G. R., Dwek, R. A., Harvey, D. J., and Zamze, S. (1998) Neutral N-glycans in adult rat brain tissue: Complete characterisation reveals fucosylated hybrid and complex structures. *Eur. J. Biochem.* 251, 691–703.
  36. Nakakita, S., Natsuka, S., Ikenaka, K., and Hase, S. (1998) Development-dependent expression of complex-type sugar chains specific to mouse brain. *J. Biochem.* 123, 1164–1168.
  37. Kitamura, N., Ikekita, M., Sato, T., Akimoto, Y., Hatanaka, Y., Kawakami, H., Inomata, M., and Furukawa, K. (2005) Mouse Na<sup>+</sup>/K<sup>+</sup>-ATPase  $\beta$ 1-subunit has a K<sup>+</sup>-dependent cell adhesion activity for  $\beta$ -GlcNAc-terminating glycans. *Proc. Natl. Acad. Sci. U.S.A.* 102, 2796–2801.

BI8009778